Discrete Heteroscorpionate Lithium and Zinc Alkyl Complexes. Synthesis, Structural Studies, and ROP of Cyclic Esters

Carlos Alonso-Moreno,[†] Andrés Garcés,[†] Luis F. Sánchez-Barba,*[,†] Mariano Fajardo,[†] Juan Fernández-Baeza,*[,‡] Antonio Otero,*[,‡] Agustín Lara-Sánchez,[‡] Antonio Antiñolo,[‡] Lewis Broomfield,[§] M. Isabel López-Solera,[‡] and Ana M. Rodríguez[‡]

Departamento de Química Inorgánica y Analítica, Universidad Rey Juan Carlos, Móstoles-28933-Madrid, Spain, Departamento de Química Inorgánica, Orgánica y Bioquímica, Universidad de Castilla-La Mancha, Campus Universitario, 13071-Ciudad Real, Spain, and Wolfson Materials and Catalysis Centre, School of Chemical Sciences and Pharmacy, University of East Anglia, Norwich, NR4 7TJ, U.K.

Received November 27, 2007

The reaction of bis(3,5-di-*tert*-butylpyrazol-1-yl)methane (bdtbpzm) with Bu^{n}Li and carbodiimide derivatives, namely, *N*,*N*′-diisopropyl and 1-*tert*-butyl-3-ethyl carbodiimides, gives rise to the new sterically hindered lithium acetamidinate [Li(tbp^{t}amd)(THF)] (**1**) [tbp^{t}amd = *N*-ethyl-*N*′-*tert*-butylbis(3,5-di-*tert*-butylpyrazol-1-yl)acetamidinate] and [Li(pbp^{t}amd)(THF)] (**2**) [pbp^{t}amd = *N*,*N*′-diisopropylbis(3,5-di-*tert*-butylpyrazol-1-yl)acetamidinate]. Subsequent hydrolysis of **1** and **2**, and the recently reported heteroscorpionate lithium salts [Li(tbpamd)(THF)] [tbpamd = *N*-ethyl-*N*′-*tert*-butylbis(3,5-dimethylpyrazol-1-yl)acetamidinate] and [Li(pbpamd)(THF)] [pbpamd = *N*,*N*′-diisopropylbis(3,5-dimethylpyrazol-1-yl)acetamidinate] with NH_4Cl/H_2O in ether cleanly affords the corresponding amidine ligands Htbpamd (**3**), Hpbpamd (**4**), Htbp^{t}amd (**5**), and Hpbp^{t}amd (**6**) in very good yields. The X-ray diffraction molecular structure of **3** was obtained. Reaction of the amidine-heteroscorpionate ligands **3**–**6** with 1 equiv of ZnR'_2 proceeds in very high yields to give the neutral heteroscorpionate alkyl zinc complexes [Zn(R′)(NNN)] (NNN = tbpamd, R′ = Me **7**, Et **8**, CH_2SiMe_3 **9**; NNN = pbpamd, R′ = Me **10**, Et **11**, CH_2SiMe_3 **12**; NNN = tbp^{t}amd, R′ = Me **13**, Et **14**; NNN = pbp^{t}amd, R′ = Me **15**, Et **16**). The single-crystal X-ray structures of the derivatives **8**, **12**, **15**, and **16** confirm a four-coordinative structure with the zinc metal center in a distorted tetrahedral geometry and the heteroscorpionate ligands arranged in κ^3-coordination mode. The new lithium salts **1** and **2** and the alkyls **7**–**9**, **13**, and **14** can act as efficient single-component initiators for the ring-opening polymerization of ϵ-caprolactone and lactides over a wide range of temperatures. ϵ-Caprolactone is polymerized within minutes to give high-medium molecular weight polymers with medium broad values of polydispersities. Lactide afforded PLA materials with medium molecular weights and polydispersities as narrow as $M_w/M_n = 1.05$. Additionally, polymerization of L-lactide occurred without racemization in the propagation process and offered highly crystalline, isotactic poly(L-lactides) with high melting temperatures ($T_m = 165$ °C). *rac*-Lactide polymerization also produces enriched levels of heterotactic poly(lactide). Polymer end group analysis shows that the polymerization mediated by alkyl zinc complexes is initiated by alkyl transfer to monomer.

Introduction

One alternative to fossil-based feedstocks[1] involves the development of chemicals from renewable resources and the development of new catalytic processes. The joint venture of Cargill−Dow in the production of the lactide monomer as a bulk commodity material represents one of the most notable recent achievements.[2] Ring-opening polymerization of lactide,[3,4] an inexpensive annually renewable natural feedstock,[5] yields polylactides, which have many properties that are similar and sometimes superior to those of traditional olefin-based polymers and have the added benefit of biodegradability.[6] In this context, zinc-based catalysts have been extensively employed in ring-opening polymerization and are among the most efficient initiators used to date for the well-controlled polymerization of cyclic esters such as ϵ-caprolactone and lactides. The biocompatible nature of these systems with living tissue and the nontoxicity of the bioassimilable polylactides (PLAs), which are also an important emerging class of environmentally friendly and recyclable thermoplastics, have attracted significant attention in biomedical and pharmaceutical applications, e.g., in resorb-

* Corresponding authors. E-mail: luisfernando.sanchezbarba@urjc.es; Antonio.Otero@uclm.es; Juan.FBaeza@uclm.es.
† Universidad Rey Juan Carlos.
‡ Universidad de Castilla-La Mancha.
§ University of East Anglia.

(1) Goodstein, D. *Out of Gas: The End of the Age of Oil*; W. W. Norton & Company: New York, 2004.
(2) (a) Gruber, P.; O'Brien, M. *Biopolymers,* **2002**, *4*, 235. (b) Drumright, R. E.; Gruber, P. R.; Henton, D. E. *Adv. Mater.* **2000**, *12*, 1841.
(3) (a) O'Keefe, B. J.; Hillmyer, M. A.; Tolman, W. B. *J. Chem. Soc., Dalton Trans.* **2001**, 2215. (b) Coates, G. W. *J. Chem. Soc., Dalton Trans.* **2002**, 467. (c) Nakano, K.; Kosaka, N.; Hiyama, T.; Nozaki, K. *Dalton Trans.* **2003**, 4039. (d) Chisholm, M. H.; Zhou, Z. *J. Mater. Chem.* **2004**, *14*, 3081.
(4) (a) Dechy-Cabaret, O.; Martin-Vaca, B.; Bourissou, D. *Chem. Rev.* **2004**, *104*, 6147. (b) Wu, J.; Yu, T-L.; Chen, C-T.; Lin, C-C. *Coord. Chem. Rev.* **2006**, *250*, 602.
(5) Biela, T.; Kowalski, A.; Libiszowski, J.; Duda, A.; Penczek, S. *Macromol. Symp.* **2006**, 47.
(6) (a) Chiellini, E.; Solaro, R. *Adv. Mater.* **1996**, *8*, 1375. (b) Ikada, Y.; Tsuji, H. *Macromol. Rapid Commun.* **2000**, *21*, 117. (c) Amgoune, A.; Thomas, C. M.; Roisnel, T.; Carpentier, J.-F. *Chem.−Eur. J.* **2006**, *12*, 169.

10.1021/om701187s CCC: $40.75 © 2008 American Chemical Society
Publication on Web 02/29/2008

able surgical sutures,[7,8] drug delivery agents,[8] and artificial tissue matrixes.[9] These medicinal applications have promoted the use of biocompatible metals. In this regard, zinc is an attractive metal. For instance, Coates, Chisholm, and Hillmyer and Tolman independently reported highly active zinc catalysts supported by sterically hindered diketiminato,[10] iminophenolato,[11] and, in particular, tris(pyrazolyl)hydroborate ligands.[12] These approaches gave high stereocontrol in the polymer microstructures as well as narrow molecular weight distributions. Stereochemistry plays a key role in PLAs, as it determines the mechanical properties, biodegradability, and, ultimately, the end use of the material.[1,6]

On the other hand, during the past decade our research group has contributed widely to the design of new "heteroscorpionate" ligands[13] related to the bis(pyrazol-1-yl)methane system,[14] with several pendant donor arms including the recently reported cyclopentadienyl[15] and amidinate[16] groups. Additionally, we have also explored the reactivity of these amidinate-based heteroscorpionate ligands as convenient ancillary ligands for the synthesis of well-defined alkyl magnesium complexes of the type [Mg(R′)(NNN)].[17] We also found that heating the monoalkyl heteroscorpionates to 90 °C in toluene results in ligand redistribution and the formation of the corresponding six-coordinate sandwich complexes [Mg(NNN)$_2$]. Moreover, heteroscorpionate magnesium alkyls proved to act as highly effective single-component living initiators for the well-controlled ring-opening polymerization of ϵ-caprolactone and lactides over a wide range of temperatures.

It is well-known that the zinc ion has filled d-orbitals and shares many similar properties, including a similar ionic radius, to the magnesium ion (Mg^{2+} = 0.71 Å, Zn^{2+} = 0.74 Å),[18] although these metals exhibit rather different chemical properties. On the basis of these similarities, we have now turned our attention to exploring the use of the same amidinate-based heteroscorpionate ligands in the synthesis of a series of alkyl zinc complexes in order to compare their synthetic accessibility, structural arrangements, and the catalytic behavior with the analogous magnesium alkyl complexes.[17] Furthermore, Gibson et al.[19] have recently highlighted the influence of the substituent on the central carbon atom of amidinate ligands to favor mono- versus bis-chelate formation amidinate complexes of magnesium and zinc. Although amidines have been extensively employed as ancillary ligands in transition metal, lanthanide, and main-group metal complexation chemistry, only a relatively small number of amidinate complexes of zinc(II) have been reported. Particularly, the only known amidinate zinc(II) complexes are either bis-chelated[20] or oxygenated tetranuclear zinc aggregates.[21]

The work described here concerns this new approach to the chemistry of these biocompatible group 2 and analogous metals, and our initial study was aimed at preparing novel organozinc complexes of the type [Zn(R′)(NNN)], where (NNN) are amidinate-based heteroscorpionates from a variety of heteroscorpionate precursors with different levels of steric congestion. The study of structural arrangements and the reactivity of these materials as single-component initiators for the ring-opening polymerization of ϵ-caprolactone and L-/*rac*-lactide under well-controlled conditions are also established.

Results and Discussion

Synthesis and Characterization of Heteroscorpionate Ligands. A mixture of a cooled (−70 °C) solution of bis(3,5-di-*tert*-butylpyrazol-1-yl)methane (bdtbpzm)[22] in THF and 1 equiv of Bu^{n}Li, under an atmosphere of dry nitrogen, was treated with the asymmetric carbodiimide *N*,*N*′-1-*tert*-butyl-3-ethylcarbodiimide and the symmetric carbodiimide *N*,*N*′-diisopropylcarbodiimide. These reactions give rise to the new sterically hindered heteroscorpionate lithium acetamidinates [Li(tbp^{t}amd)(THF)] (**1**) [tbp^{t}amd = *N*-ethyl-*N*′-*tert*-butylbis(3,5-di-*tert*-butylpyrazol-1-yl)acetamidinate] and [Li(pbp^{t}amd)(THF)] (**2**) [pbp^{t}amd = *N*,*N*′-diisopropylbis(3,5-di-*tert*-butylpyrazol-1-yl)acetamidinate] as white solids in good yield (ca. 85%) after the appropriate workup (Scheme 1). Subsequent hydrolysis of the recently reported less sterically congested heteroscorpionate lithium salts [Li(tbpamd)(THF)][16] [tbpamd = *N*-ethyl-*N*′-*tert*-butylbis(3,5-dimethylpyrazol-1-yl)acetamidinate] and [Li(pbpamd)(THF)][16] [pbpamd = *N*,*N*′-diisopropylbis(3,5-dimethylpyrazol-1-yl)acetamidinate] and the much more sterically hindered [Li(tbp^{t}amd)(THF)] (**1**) and [Li(pbp^{t}amd)(THF)] (**2**) with NH_4Cl/H_2O in diethyl ether cleanly affords the corre-

(7) (a) Schmitt, E. E.; Polistina, R. A. U.S. Patent 3,463,158, 1969. (b) Frazza, E. J.; Schmitt, E. E. J. *Biomed. Mater. Res. Symp.* **1971**, *1*, 43. (c) Dexon and Vicryl are products of Davis & Geek Corp., Wayne, NJ, and Ethicon, Inc., Somerville, NJ, respectively.

(8) (a) Leupron Depot is a product of Takeda Chemical Industries, Ltd., Japan, for drug delivery purposes. (b) *Taehan Hwakakhoe Chi* **1990**, *34*, 203; *Chem. Abstr.* **1990**, *113*, 98014g.

(9) (a) Hubbell, J. A.; Langer, R. *Chem. Eng. News* **1995**, *Mar 13*, 42. (b) Langer, R.; Vacanti, J. *P. Science* **1993**, *260*, 920. (c) Chisholm, M. H.; Iyer, S. S.; McCollum, D. G.; Pagel, M.; Werner-Zwanziger, U. *Macromolecules* **1999**, *32*, 963.

(10) (a) Chen, M.; Attygalle, A. B.; Lobkovsky; E. B.; Coates, G. W. *J. Am. Chem. Soc.* **1999**, *121*, 11583. (b) Chamberlain, B. M.; Cheng, M.; Moore, D. R.; Ovitt, E. B.; Lobkovsky, E. B.; Coates, G. W. *J. Am. Chem. Soc.* **2001**, *123*, 3229. (c) Chisholm, M. H.; Galluci, J.; Zhen, H.; Huffman, J. C. *Inorg. Chem.* **2001**, *40*, 5051. (d) Chisholm, M. H.; Galluci, J.; Phomphrai, K. *Inorg. Chem.* **2002**, *41*, 2785.

(11) Williams, C. K.; Breyfogle, L. E.; Choi, S. K.; Nam, W.; Young, V. G., Jr; Hillmyer, M. A.; Tolman, W. B. *J. Am. Chem. Soc.* **2003**, *125*, 11350.

(12) (a) Chisholm, M. H.; Eilerts, N. W. *Chem. Commun.* **1996**, 853. (b) Chisholm, M. H.; Eilerts, N. W.; Huffman, J. C.; Iyer, S. S.; Pacold, V.; Phomphrai, K. *J. Am. Chem. Soc.* **2000**, *122*, 11845.

(13) Trofimenko, S. *Scorpionates. The Coordination Chemistry of Polypyrazolylborate Ligands*; Imperial College Press: London, 1999.

(14) (a) Otero, A.; Fernández-Baeza, J.; Antiñolo, A.; Tejeda, J.; Lara-Sánchez, A. *Dalton Trans.* **2004**, 1499. (b) Pettinari, C.; Pettinari, R. *Coord. Chem. Rev.* **2005**, *249*, 525. (c) Pettinari, C.; Pettinari, R. *Coord. Chem. Rev.* **2005**, *249*, 663. (d) Bigmore, H. R.; Lawrence, S. C.; Mountford, P.; Tredget, C. S. *Dalton Trans.* **2005**, 635.

(15) (a) Otero, A.; Fernández-Baeza, J.; Antiñolo, A.; Tejeda, J.; Lara-Sánchez, A.; Sánchez-Barba, L.; Rodríguez, A. M.; Maestro, M. A. *J. Am. Chem. Soc.* **2004**, *126*, 1330. (b) Otero, A.; Fernández-Baeza, J.; Antiñolo, A.; Tejeda, J.; Lara-Sánchez, A.; Sánchez-Barba, L. F.; Sánchez-Molina, M.; Rodríguez, A. M.; Bo, C.; Urbano-Cuadrado, M. *Organometallics* **2007**, *26*, 4310.

(16) Otero, A.; Fernández-Baeza, J.; Antiñolo, A.; Tejeda, J.; Lara-Sánchez, A.; Sánchez-Barba, L. F.; López-Solera, I.; Rodríguez, A. M. *Inorg. Chem.* **2007**, *46*, 1760 and references therein.

(17) Sánchez-Barba, L. F.; Garcés, A.; Fajardo, M.; Alonso-Moreno, C.; Fernández-Baeza, J.; Otero, A.; Antiñolo; A.; Tejeda, J.; Lara-Sánchez; A.; López-Solera, M. I. *Organometallics* **2007**, *26*, 6403.

(18) Cotton, F. A.; Wilkinson, E.; Murillo, C. A.; Bochmann, M. *Advanced Inorganic Chemistry*, 6th ed.; Wiley and Sons: New York, 1999; p 1302.

(19) Nimitsiriwat, N.; Gibson, V. C.; Marshall, E. L.; Takolpuckdee, P.; Tomov, A. K.; White, A. J. P.; Williams, D. J.; Elsegood, M. R. J.; Dale, S. H. *Inorg. Chem.* **2007**, *46*, 9988.

(20) (a) Buijink, J. K.; Noltemeyer, M.; Edelmann, F. T. *Z. Naturforsch.* **1991**, *46*, 1328–1332. (b) Edelmann, F. T. *Coord. Chem. Rev.* **1994**, *137*, 403.

(21) (a) Cotton, F. A.; Daniels, L. M.; Falvello, L. R.; Matonic, J. H.; Murillo, C. A.; Wang, X.; Zhou, H. *Inorg. Chim. Acta* **1997**, *266*, 91. (b) Cole, M. L.; Evans, D. J.; Junk, P. C.; Louis, L. M. *New J. Chem.* **2002**, *26*, 1015.

(22) Beck, A.; Weibert, B.; Burzlaff, N. *Eur. J. Inorg. Chem.* **2001**, 521.

Scheme 1. Synthesis of the Lithium Salts 1 and 2 and the Corresponding Amidine-Heteroscorpionate Ligands 3–6

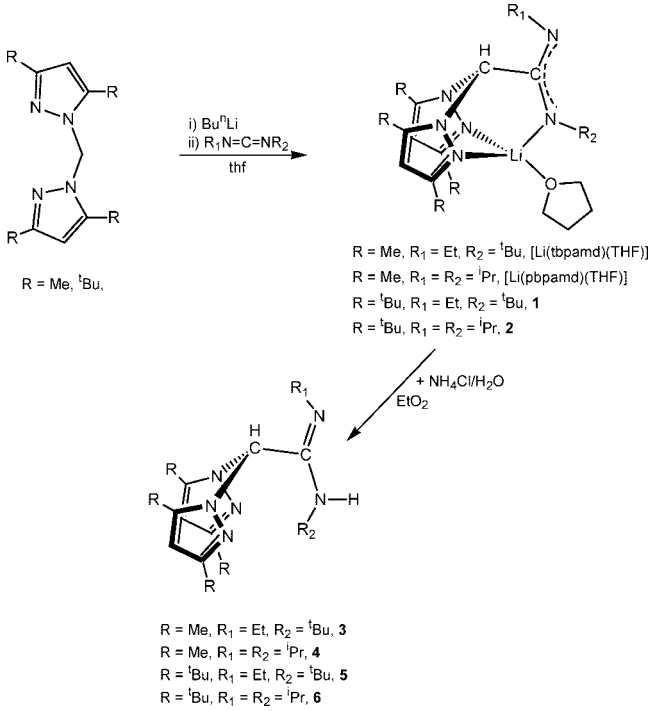

sponding amidine ligands Htbpamd (**3**), Hpbpamd (**4**), Htbp^{t}amd (**5**), and Hpbp^{t}amd (**6**) in very good yields (Scheme 1).

The ^{1}H and ^{13}C{^{1}H} NMR spectra of the new lithium salts **1** and **2** in benzene-d_6 at room temperature display a single set of resonances for the pyrazole rings, indicating that both pyrazole rings are equivalent. These data confirm a tetrahedral disposition of the lithium atom with NNN-coordination for the heteroscorpionate ligand, where a symmetric plane exists that contains the amidinate group and the THF ligand (Scheme 1). The NMR spectra for the amidinate moiety of the lithium compound **2** (in which $R_1 = R_2 = {}^i$Pr) show two set of resonances for these substituents. These data are indicative of monodentate binding of the amidinate moiety to the lithium atom, a phenomenon that has previously been observed for the derivative [Li(pbpamd)(THF)]. ^{1}H NOESY-1D experiments were also performed in order to confirm the assignment of the signals for the ^{t}Bu^3, ^{t}Bu^5, and H^4 groups. Furthermore, in compound **1** (where $R_1 \neq R_2$) the response in the ^{1}H NOESY-1D experiment from ^{t}Bu^5 protons of the pyrazolyl rings on irradiating the ethyl group of the amidinate moiety suggests that this group is in the position R_1, whereas the *tert*-butyl group is in R_2 (see Scheme 1). ^{1}H−^{13}C heteronuclear correlation (gHSQC) experiments were carried out and allowed us to assign the resonances corresponding to C^4, ^{t}Bu^3, and ^{t}Bu^5 of the pyrazole ring. Finally, the ^{7}Li NMR spectra of these compounds exhibit a singlet at δ = 1.61–1.63 ppm for the lithium atom. The mass spectra (FAB) of these compounds indicate a mononuclear formulation (see Experimental Section). In addition, the ^{1}H and ^{13}C{^{1}H} NMR spectra of the amidine-heteroscorpionate compounds **3–6** in benzene-d_6 at room temperature show a single set of resonances for the pyrazole rings, indicating that both pyrazoles are equivalent (Scheme 1).

The molecular structure of Htbpamd (**3**) was confirmed by single-crystal X-ray diffraction studies and is depicted in Figure 1. Significant bond distances and bond angles are listed in Table 1. Whereas the C(12)−N(5) distance found in this compound [1.270(2) Å] is typical of C=N double bonds, as in Schiff bases

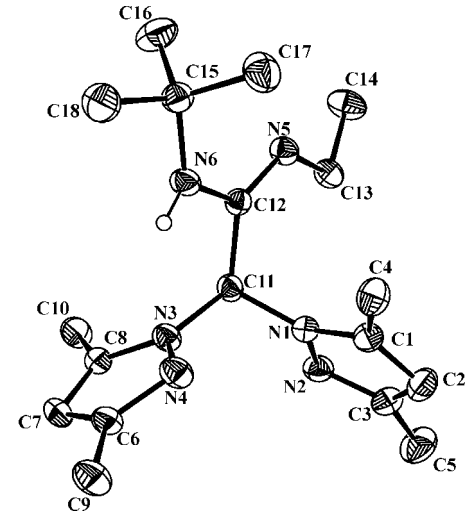

Figure 1. ORTEP view of [Htbpamd] (**3**). Hydrogen atoms have been omitted for clarity. Thermal ellipsoids are drawn at the 30% probability level.

and oximes (ca. 1.26 Å), the C(12)−N(6) (1.361 Å) bond length is typical of a C−N single bond. The hydrogen atom is located on the N atom bonded to the ^{t}Bu substituent, i.e., the more sterically hindered amino group. The essentially sp^2 and planar nature of the imino carbon atom C(12) is further confirmed by the summations of the angles around it (360°).

Synthesis and Characterization of Alkyl Zinc Complexes. Given that simple Zn(II) salts suffer from low reactivity, limited solubility, and solution aggregation phenomena that complicate mechanistic analysis (e.g., non-first-order kinetic dependencies on catalyst concentration),[23,11] and considering our previous experience in the synthesis of the analogous magnesium derivatives,[17] we decided to react the amidine-heteroscorpionate ligands **3–6** with ZnR′$_2$ (1 equiv vs Zn) at low temperature to afford cleanly the corresponding neutral monoalkyl heteroscorpionate zinc complexes [Zn(R′)(NNN)] (NNN = tbpamd, R′ = Me **7**, Et **8**, CH_2SiMe_3 **9**; pbpamd, R′ = Me **10**, Et **11**, CH_2SiMe_3 **12**; tbp^{t}amd, R′ = Me **13**, Et **14**; pbp^{t}amd, R′ = Me **15**, Et **16**) in very good yields (>75%) as white microcrystalline powders (Scheme 2). Attempts to prepare zinc alkyl derivatives with NNN = tbp^{t}amd or pbp^{t}amd and R′ = CH_2SiMe_3 failed, possibly due to the higher level of congestion created around the metal coordination sphere. The compounds synthesized are extremely air- and moisture-sensitive, highly soluble in THF, toluene, and diethyl ether, but sparingly soluble in *n*-hexane, apart from derivatives with R = ^{t}Bu. The complexes decompose in dichloromethane. The synthesis of equivalent homoscorpionate tris(pyrazolyl)phenylborate four-coordinate zinc alkyl complexes was previously reported in the excellent pioneering work of Parkin and Vahrenkamp et al.[24] A metathetical reaction between $ZnEt_2$ and thallium(I) tris(pyrazolyl)phenylborates was used in a similar

(23) Kowalski, A.; Duda, A.; Penczek, S. *Macromolecules* **1998**, *31*, 2114, and references therein.

(24) (a) Looney, A.; Han, R.; Gorrell, I. B.; Cornebise, M.; Yoon, K.; Parkin, G.; Rheingold, A. L. *Organometallics* **1995**, *14*, 274. (b) Gorrell, I. B.; Looney, A.; Parkin, G. *J. Chem. Soc., Chem. Commun.* **1990**, 220. (c) Alsfasser, R.; Powell, A. K.; Vahrenkamp, H. *Angew. Chem., Int. Ed. Engl.* **1990**, *29*, 898. (d) Alsfasser, R.; Powell, A. K.; Trofimenko, S.; Vahrenkamp, H. *Chem. Ber.* **1993**, *126*, 685. (e) Kisko, J. L.; Fillebeen, T.; Hascall, T.; Parkin, G. *J. Organomet. Chem.* **2000**, *596*, 22.

Table 1. Selected Interatomic Distances (Å) and Angles (deg) for 3, 8, 12, 15, and 16[a]

3		8		12		15		16	
C(12)−N(5)	1.270(2)	Zn(1)−N(1)	2.131(3)	Zn(1)−N(1)	2.158(4)	Zn(1)−N(1)	2.236(3)	Zn(1)−N(1)	2.134(3)
C(12)−N(6)	1.361(3)	Zn(1)−N(3)	2.121(2)	Zn(1)−N(3)	2.157(4)	Zn(1)−N(3)	2.118(3)	Zn(1)−N(3)	2.225(3)
C(11)−N(3)	1.452(3)	Zn(1)−N(5)	1.986(2)	Zn(1)−N(5)	1.981(4)	Zn(1)−N(5)	2.003(3)	Zn(1)−N(5)	1.997(3)
C(11)−N(1)	1.442(3)	Zn(1)−C(19)	1.973(2)	Zn(1)−C(19)	1.992(5)	Zn(1)−C(31)	1.968(3)	Zn(1)−C(1)	1.995(4)
		N(6)−C(12)	1.293(4)	N(6)−C(1)	1.290(6)	N(6)−C(24)	1.308(4)	N(6)−C(3)	1.307(4)
		N(5)−C(12)	1.351(4)	N(5)−C(1)	1.354(6)	N(5)−C(24)	1.340(4)	N(5)−C(3)	1.346(4)
N(3)−C(11)−N(1)	111.4(2)	N(3)−Zn(1)−N(1)	85.1(1)	N(3)−Zn(1)−N(1)	83.2(1)	N(3)−Zn(1)−N(1)	82.2(1)	N(3)−Zn(1)−N(1)	80.5(1)
N(6)−C(12)−N(5)	122.5(2)	N(3)−Zn(1)−N(5)	90.9(1)	N(3)−Zn(1)−N(5)	91.9(1)	N(3)−Zn(1)−N(5)	91.5(1)	N(3)−Zn(1)−N(5)	92.9(1)
N(6)−C(12)−C(11)	114.4(2)	N(1)−Zn(1)−N(5)	90.2(1)	N(1)−Zn(1)−N(5)	89.0(1)	N(1)−Zn(1)−N(5)	93.3(1)	N(1)−Zn(1)−N(5)	91.7(1)
N(5)−C(12)−C(11)	123.0(2)	N(5)−Zn(1)−C(19)	142.3(1)	N(5)−Zn(1)−C(19)	145.7(2)	N(5)−Zn(1)−C(31)	128.9(1)	N(5)−Zn(1)−C(1)	131.0(1)
		C(12)−N(5)−C(15)	118.1(2)	C(1)−N(5)−C(16)	115.2(4)	C(25)−N(5)−C(24)	122.1(3)	C(3)−N(5)−C(8)	121.2(3)

[a] Symmetry transformation used to generate equivalent atom: $-x + 1, -y, -z$.

Scheme 2. Synthesis of the Heteroscorpionate Alkyl Zinc Complexes [Zn(R′)(NNN)] (7–16)

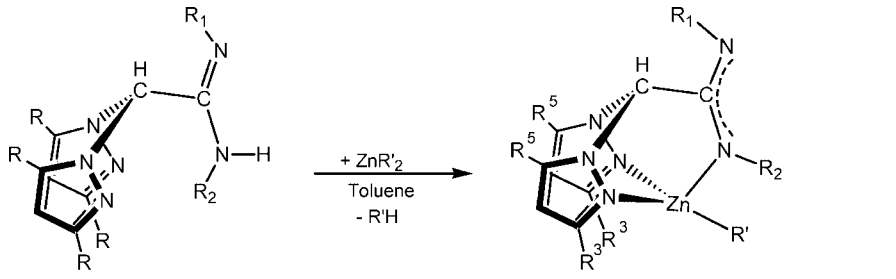

(**3**-**6**)

R = Me, R_1 = Et, R_2 = ^{t}Bu, R' = Me **7**, Et **8**, CH_2SiMe_3 **9**
R = Me, R_1 = R_2 = ^{i}Pr, R' = Me **10**, Et **11**, CH_2SiMe_3 **12**
R = ^{t}Bu, R_1 = Et, R_2 = ^{t}Bu, R' = Me **13**, Et **14**
R = ^{t}Bu, R_1 = R_2 = ^{i}Pr, R' = Me **15**, Et **16**

Table 2. Polymerization of ϵ-Caprolactone Catalyzed by Complexes 1–2 and 7–9[a]

entry	initiator	$[\epsilon\text{-CL}]_0/[\text{initiator}]_0$	temp (°C)	time (min)	yield (g)	conv (%)[b]	prod[c]	M_w (Da)[d]	M_w/M_n[d]
1	**1**	500	20	45	4.58	92	68	65 400	1.56
2	**1**	5000[e]	20	120	7.41	67	185	157 000	1.67
3	**2**	500	20	45	4.83	97	71	58 000	1.55
4	**2**	500	0	30	2.58	52	57	51 000	1.33
5	**2**	500	70	2	4.88	98	1 626	131 300	2.07
6	$[Mg(CH_2SiMe_3)(tbpamd)]$[f]	500	20	1	4.98	97	3 320	52 000	1.41
7	**7**	500	85	110	4.48	90	27	63 000	1.43
8	**7**	500	65	110	traces				
9	**8**	500	85	110	4.78	96	28	71 000	1.42
10	**8**	500	65	110	1.24	25	7	42 000	1.23
11	**9**	500	20	15(h)	1.19	24	1	20 300	1.09
12	**9**	500	50	15(h)	2.24	45	1	29 100	1.67
13	**9**	500	85	40	4.83	97	80	167 000	1.82
14	**9**	5000[e]	85	120	4.64	42	116	192 000	1.72

[a] Polymerization conditions: 90 μmol of initiator. [b] Percentage conversion of the monomer (weight of polymer recovered/weight monomer × 100). [c] kg polymer·[mol of metal (Li/Zn)]$^{-1}$·h^{-1}. [d] Determined by GPC relative to polystyrene standards in tetrahydrofuran. [e] 20 μmol of initiator. [f] These data have been included for comparison in ROP with the alkyl zinc analogues.[17]

synthetic procedure employed to prepare analogous magnesium alkyl complexes from MgR_2.[25]

The ^{1}H and ^{13}C{^{1}H} NMR spectra of **7–16** in benzene-d_6 at room temperature display a single set of resonances for the pyrazole rings, indicating that both pyrazole rings are equivalent. These data suggest a tetrahedral disposition for the zinc atom with NNN-coordination of the heteroscorpionate ligand, a situation in which a plane of symmetry exists and contains both the amidinate group and the alkyl ligand (Scheme 2). The NMR signals due to the amidinate moiety of the zinc compounds **10–12** and **15–16** (where $R_1 = R_2 = {}^i$Pr) show two sets of resonances for these substituents in a similar way to the precursor lithium salt **2**. This observation is indicative of monodentate binding of the amidinate moiety to the zinc atom. Additionally, ^{1}H NOESY-1D experiments were also performed to confirm the assignment of the signals for the $Me^{3\text{ or }5}$, $^tBu^{3\text{ or }5}$, and H^4 groups of the pyrazole rings. Furthermore, for compounds **7–9** and **13–14** (where $R_1 \neq R_2$), the response in the ^{1}H NOESY-1D experiment from the Me^5 and $^tBu^5$ protons of the pyrazole rings on irradiation of the ethyl group of the amidinate moiety suggests that this group is in the R_1 position, whereas the *tert*-butyl group is in the R_2 position (Scheme 2), as in the lithium salt **1**.

X-ray Crystal Structures of Alkyl Heteroscorpionate Zinc Complexes. Complexes **8**, **12**, **15**, and **16** were characterized by single-crystal X-ray diffraction studies. Selected bond lengths and angles are collected in Table 1. Crystallographic details are reported in Table 4 and the molecular structures are shown in Figures 2 through 5, respectively. All of the zinc complexes have a monomeric structure in the solid state, and the zinc center exhibits a distorted tetrahedral geometry, in which the pyrazolic nitrogens N(1) and N(3) occupy two positions and

(25) (a) Han, R.; Looney, A.; Parkin, G. *J. Am. Chem. Soc.* **1989**, *111*, 7276. (b) Han, R.; Parkin, G. *J. Am. Chem. Soc.* **1990**, *112*, 3662. (c) Han, R.; Brachrach, M.; Parkin, G. *Polyhedron* **1990**, *9*, 1775. (d) Han, R.; Parkin, G. *Organometallics* **1991**, *10*, 1010.

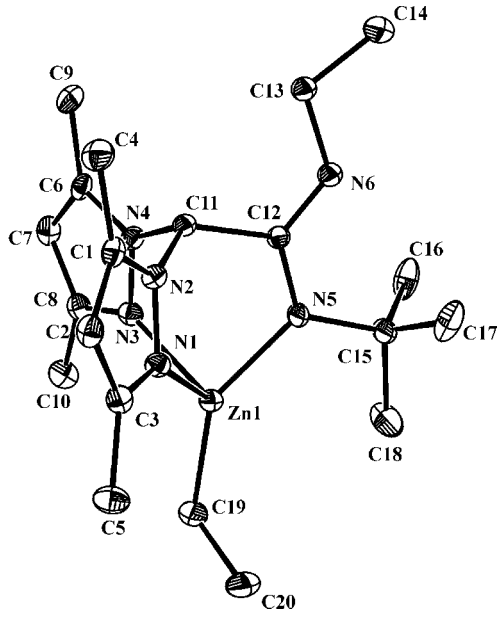

Figure 2. ORTEP view of [Zn(CH_2CH_3)(tbpamd)] (**8**). Hydrogen atoms have been omitted for clarity. Thermal ellipsoids are drawn at the 30% probability level.

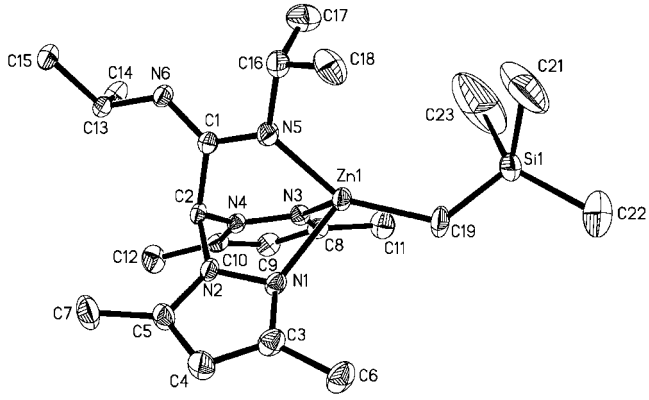

Figure 3. ORTEP view of [Zn(CH_2SiMe_3)(pbpamd)] (**12**). Hydrogen atoms have been omitted for clarity. Thermal ellipsoids are drawn at the 30% probability level.

the amidinate nitrogen N(5) and the alkyl group the other two positions. The solid-state structure also confirms that in all cases the amidinate fragment is coordinated in a monodentate fashion to the Zn atom, a situation that is relatively unusual,[16,17,26] and delocalization is also evidenced in the N−C−N core of the amidinate, with the bond lengths C−N(6) and C−N(5) ranging on average from 1.290(6) to 1.354(6) Å.

The molecular structure of **8** (Figure 2) shows a distortion of the metal center due to the heteroscorpionate ligand, which acts in an NNN coordination mode with the N(1)−Zn and N(3)−Zn bond lengths well balanced [2.131(3) and 2.121(3) Å] (Table 1) and comparable to that observed in analogous alkyl magnesium[17] complexes [N(2)−Mg = 2.126(3) Å and N(3)−Mg = 2.122(3) Å]. The four-membered Zn−N(5)−C(12)−C(11) fragment and the ethyl group lie around a mirror plane that shows the symmetry in the molecule. The N(5)−Zn bond length

(26) (a) Grove, D. M.; van Koten, G.; Ubbels, H. J. C.; Vrieze, K.; Niemann, L. C.; Stam, C. H. *J. Chem. Soc., Dalton Trans.* **1986**, 717. (b) Zinn, A.; Dehnicke, L.; Fenske, D.; Baum, G. Z. *Anorg. Allg. Chem.* **1991**, *596*, 47. (c) Foley, S. R.; Bensimon, C.; Richeson, D. S. *J. Am. Chem. Soc.* **1997**, *119*, 10359.

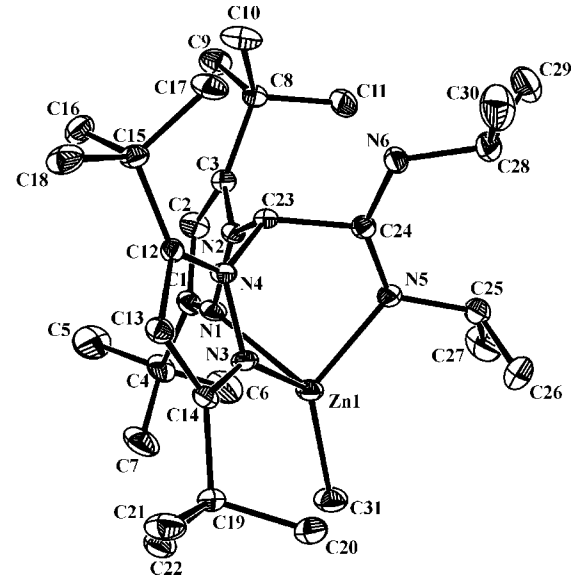

Figure 4. ORTEP view of [Zn(CH_3)(pbp^{t}amd)] (**15**). Hydrogen atoms have been omitted for clarity. Thermal ellipsoids are drawn at the 30% probability level.

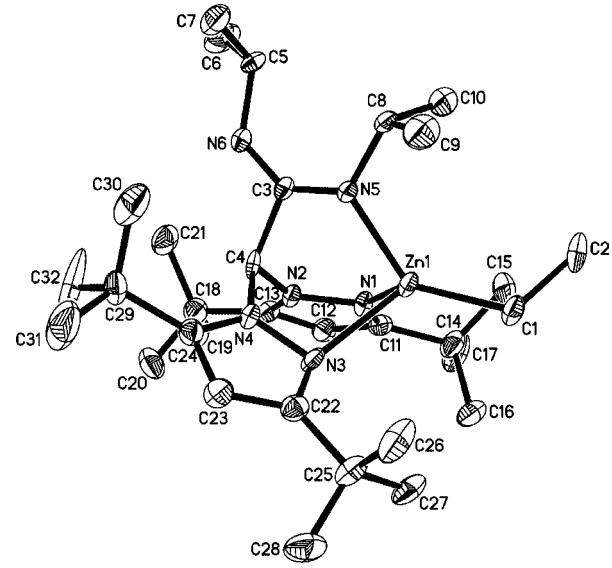

Figure 5. ORTEP view of [Zn(CH_2CH_3)(pbp^{t}amd)] (**16**). Hydrogen atoms have been omitted for clarity. Thermal ellipsoids are drawn at the 30% probability level.

[1.986(2) Å] is shorter than the N(1)− and N(3)−Zn bond lengths. Finally, the ethyl moiety is directly bonded to the Zn center with a Zn−C(19) bond length of 1.973(3) Å, showing essentially sp^3 hybridization, as evidenced by the angle Zn−C(19)−C(20) = 118.1(2)°.

The crystal structure of complex **12** (Figure 3) shows N(1)−Zn and N(3)−Zn bond lengths [2.158(4) and 2.157(4) Å] longer than those observed in complex **8** [N(1)−Zn = 2.131(3) Å and N(3)−Zn = 2.121(3) Å] (Table 1).

The N(5)−Zn bond length [1.981(4) Å] is comparable to that in complex **8** [1.986(2) Å]. The Zn−C(19) bond length [1.992(5) Å] in the alkyl moiety in the solid state is longer than that in the ethyl group in complex **8** [Zn−C(19) = 1.973(2) Å] as a result of the sterical hindrance of the alkyl group CH_2SiMe_3.

Interestingly, in the X-ray molecular structures of complexes **15** and **16** (Figures 4 and 5, respectively), the N(1)−Zn and N(3)−Zn bond lengths are not very similar in these sterically

Table 3. Polymerization of L-Lactide and *rac*-Lactide Catalyzed by Complexes 1, 8, 13, and 14[a]

entry	initiator	monomer	temp (°C)	time (h)	yield (g)	conv (%)[b]	M_n (Da)[c]	M_w/M_n[c]	T_m (°C)[d]	$[\alpha]_D^{22}$ (deg)[e]	P_r[f]
1	**1**	L-LA	110	10	0.29	23	6 500	1.28	155	−146	
2	**1**	L-LA	110	36	1.18	92	14 000	1.35	154	−147	
3	**1**	L-LA	bulk	0.75	1.16	90	14 500	1.45	156	−148	
4	**13**	L-LA	110	24	0.55	43	6 500	1.05	165	−145	
5	**13**	L-LA	110	36	0.89	69	9 500	1.09	164	−145	
6	**13**	L-LA	110	48	1.04	81	11 200	1.08	165	−144	
7	**14**	L-LA	110	48	0.98	76	11 000	1.09	162	−142	
8	$[Mg(CH_2SiMe_3)(tbpamd)]$[g]	*rac*-LA	70	72	0.41	31	5 900	1.09	121		atactic
9	**8**	*rac*-LA	110	48	0.83	65	9 700	1.14	111		atactic
10	**13**	*rac*-LA	110	24	0.42	33	5 400	1.08	125		0.62
11	**13**	*rac*-LA	110	48	0.91	71	10 600	1.13	129		0.60
12	**13**	*rac*-LA	bulk	0.75	0.78	61	8 300	1.43	132		0.50
13	**14**	*rac*-LA	110	48	0.81	63	8 700	1.11	125		0.68
14	**14**	*rac*-LA[h]	110	48	1.14	89	13 400	1.23	134		0.60

[a] Polymerization conditions: 90 μmol of initiator; $[\text{L-lactide}]_0/[\text{initiator}]_0 = 100$ and $[\textit{rac}\text{-LA}]_0/[\text{initiator}]_0 = 100$, in toluene. [b] Percentage conversion of the monomer (weight monomer/weight of polymer recovered × 100). [c] Determined by GPC relative to polystyrene standards in tetrahydrofuran. [d] PLA melting temperature. [e] Optical rotation data of poly(L-lactide) obtained. $[\alpha]_D^{22}$ of L-lactide and poly(L-lactide) are −285° and −144°, respectively.[12b] [f] P_r is the probability of racemic linkages between monomer units and is determined from the relative intensity of the *sis* (δ 5.22 ppm) and *isi* (δ 5.15 ppm) tetrads vs other tetrads (*iis*/*sii*, δ 5.21 and 5.175 ppm; *iii*, δ 5.16 ppm) × 100.[43] [g] These data have been included for comparison in ROP with the alkyl zinc analogues.[17] [h] Addition of ^{i}PrOH to the precatalyst in a ratio of 1:1.

hindered ligands, as evidenced in the values for N(1)−Zn = 2.236(3) Å and N(3)−Zn = 2.118(3) Å for **15** and N(1)−Zn = 2.134(3) Å and N(3)−Zn = 2.225(3) Å for **16**.

The N(5)−Zn bond lengths for **15** [2.003(3) Å] and **16** [1.997(3) Å] are comparable and are consistently longer than those observed in the isopropyl-containing amidinate fragment in complex **12** [1.981(4) Å]. This difference is a consequence of the greater steric demand of the ligand in the former complexes. Finally, the high level of steric hindrance exerted by this heteroscorpionate ligand (pbp^{t}amd) is also manifested in the Zn−C bond length, which is notably longer in complex **16** [Zn−C(1) = 1.995(4) Å] than in complex **8** [Zn−C(19) = 1.973(3) Å].

In view of the fact that Grignard reagents exist in solution as a complex mixture of species due to facile ligand redistribution reactions, e.g., the Schlenk equilibrium,[27] we investigated the possibility of similar ligand-exchange processes for the heteroscorpionate alkyl zinc complexes synthesized here, [Zn(R′)(NNN)] (**7**–**16**), in order to prepare the corresponding potential six-coordinate sandwich species of the type $[Zn(NNN)_2]$. This behavior has previously been observed by Parkin[28] in similar alkyl homoscorpionate magnesium complexes and by our group in alkyl heteroscorpionate magnesium complexes.[17] The formation of zinc sandwich complexes from heteroscorpionates based on a carboxylate system has also been described by Burzlaff,[22] and species of stoichiometry $[ZnL_2]$ in a tetrahedral arrangement based on sulfur donor atoms have also been reported by Carrano.[29] It is worth noting that solutions of derivatives **7**–**16** are stable in refluxing toluene during days, and a ligand redistribution process to give the six-coordinate sandwich complexes $[Zn(NNN)_2]$ was not observed in any case. Furthermore, when the reaction was carried out with 2 equiv of ligand versus Zn, even under reflux in toluene, formation of the sandwich species was not detected.

Polymerization Studies. Complexes **1**, **2**, **7**–**9**, **13**, and **14** were assessed in the ring-opening polymerization of the polar monomers ϵ-caprolactone (CL) and L-/*rac*-lactide (L-LA, *rac*-LA).

ϵ-Caprolactone Polymerization Promoted by Lithium and Zinc Alkyl Heteroscorpionate Complexes. Initiators **1** and **2** and **7**–**9** act as efficient single-component catalysts for the polymerization of ϵ-caprolactone (CL) to give high-medium molecular weight polymers; the results of these experiments are collected in Table 2. A variety of polymerization conditions were explored. The heteroscorpionate lithium salts **1** and **2** initiate very rapid polymerization of CL at room temperature (entries 1 and 3), and **2** gives almost complete conversion of 500 equiv of CL in 45 min, with a productivity of more than 7×10^4 g PCL (mol Li)$^{-1}\cdot$h^{-1}. The polymerization gives a medium molecular weight polymer with medium broad values of polydispersity (for example, $M_w = 58\,000$, $M_w/M_n = 1.55$). This activity is maintained at 0 °C (entry 4), and in 30 min 52% of the monomer was converted with $M_w/M_n = 1.33$. Not unexpectedly, an increase in the temperature up to 70 °C led to complete conversion of the monomer in 2 min with a high polydispersity index ($M_w/M_n = 2.07$, entry 5), showing a higher productivity [162×10^4 g PCL (mol Li)$^{-1}\cdot$h^{-1}]. To the best of our knowledge, examples of heteroscorpionate lithium salts have not been reported previously for the ring-opening polymerization of ϵ-caprolactone.[4b]

Alkyl initiators **7**–**9** showed lower activity than the precursors **1** and **2** and much lower activity than the analogous heteroscorpionate alkyl magnesium derivatives recently reported by our group[17] (Table 2, entry 6). For example, **7** and **8** polymerize CL effectively at 85 °C (entries 7 and 9) and **8** gives almost complete conversion of 500 equiv of CL in 110 min, with a productivity of more than 2×10^4 g PCL (mol Zn)$^{-1}\cdot$h^{-1}. The productivity and molecular weight decrease markedly on cooling (entries 8 and 10), and in the reaction at 65 °C, 25% of the polymer is recovered for **8**, with a low index of polydispersity ($M_w/M_n = 1.23$, entry 10), whereas **7** drastically reduces the catalytic activity at the same temperature and only traces of product are formed (entry 8). Interestingly, complex **9** showed a very high activity in comparison with the Me- and Et-containing derivatives, and at room temperature 24% of the monomer was transformed after 15 h to give a narrow molecular weight distribution ($M_w/M_n = 1.09$, entry 11). As expected, increases in the temperature produced higher molecular weight polymers as well as higher values of polydispersities ($M_w/M_n = 1.82$, entry 13).

(27) Ashby, E. C. *Pure Appl. Chem.* **1980**, *52*, 545.
(28) Han, R.; Parkin, G. *J. Am. Chem. Soc.* **1992**, *114*, 748.
(29) (a) Hammes, B. S.; Carrano, C. *J. Inorg. Chem.* **1999**, *38*, 4593. (b) Hammes, B. S.; Carrano, C. J. *J. Chem. Soc., Dalton Trans.* **2000**, 3304.

Scheme 3. Possible Mechanisms for the Ring-Opening Polymerization of Cyclic Esters

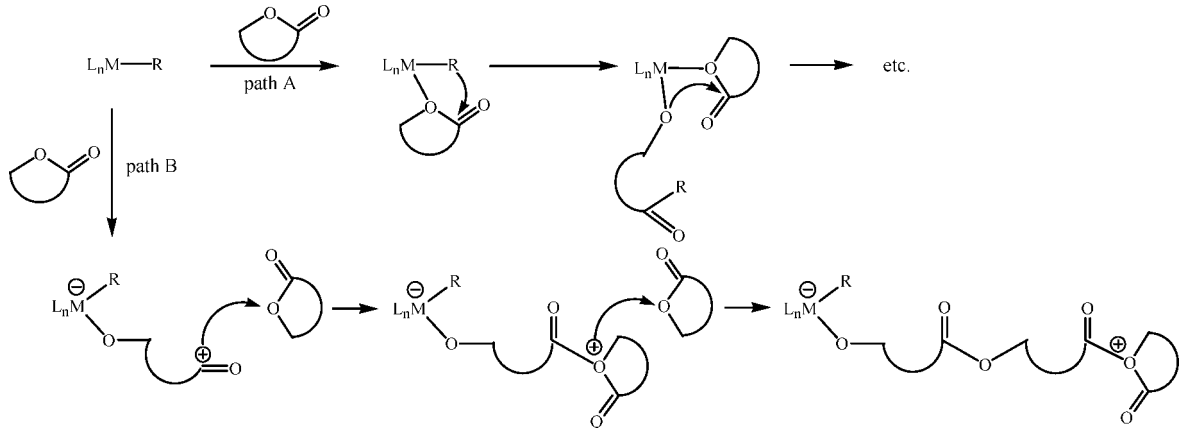

In these tests the polymer molecular weights were limited by a monomer/initiator ratio of 500:1. Increasing this ratio by a factor of 10 gave polymers with significantly higher molecular weights ($M_w > 10^5$) and broader molecular weight distributions (entries 2 and 14). Two possibilities can account for the relatively broad polydispersities observed with complexes **7–9** in comparison with the magnesium analogues:[17] (1) the use as an initiator of a Zn-alkyl group, which is known to be less nucleophilic than alkoxides, leads to a delay in comparison to propagation[30] and (2) back-biting reaction/transesterification take place as side reactions, resulting in the formation of macrocycles with a wide range of molecular weight distributions.

The lithium salts **1** and **2** are significantly more active initiators than the alkyl zinc complexes **7–9**. This marked difference in reactivity between the two types of species is presumably a consequence of the fundamental mechanistic differences in their polymerization performances.[4b] In most cases, it has been established that polymerization can be envisaged to occur by one of two mechanisms: either transfer of the nucleophilic alkyl ligand to the monomer, with formation of a metal alkoxide-propagating species (Scheme 3, path A),[31] or ring-opening and propagation through a cationic (activated chain end, ACE) mechanism (path B).[32]

End group analysis of the polymers obtained from **1** and **2** reveals the absence of the heteroscorpionate ligand in the ^{1}H NMR spectrum, and in agreement with the results, an insertion mechanism must be excluded (path A). Alternatively, a cationic (activated chain end, ACE) mechanism (Scheme 3, path B) could be considered, where a carbocationic species is initially formed, followed by a propagation step. However, in the absence of experimental data for the formation of the hypothetical carbocationic intermediate from MALDI-TOF-MS spectrometric measurements, other proposals such as an intramolecular cyclization cannot be ruled out.

By contrast, end group analysis for the polymerization catalyzed by **9** shows that the polymer contains $-CH_2SiMe_3$ termini, which provides evidence confirming that the polymerization follows a nucleophilic route and is initiated by the transfer of an alkyl ligand to the monomer, with cleavage of the acyl−oxygen bond and formation of a metal alkoxide-propagating species.[31] Very few alkyl zinc initiators[33] have been shown to polymerize ϵ-caprolactone to medium molecular weight polymers. By contrast, catalysts **7–9** proved to be efficient initiators for the production of high-medium molecular weight polymers with medium broad molecular weight distributions, even at a catalyst loading of 0.08%, which yielded M_n values as high as 112 kg·mol^{-1} (entry 14).

L- and *rac*-Lactide Polymerization Initiated by Lithium and Zinc Alkyl Heteroscorpionate Complexes. Several alkali metal compounds such as butyllithium, lithium *tert*-butoxide, and potassium *tert*-butoxide have been used to polymerize L-lactide and *rac*-lactide by Kricheldorf and Kasperczyk et al.[34] These compounds are effective initiators, although the high basicity of these ionic species results in detrimental side reactions such as epimerization of chiral centers in the PLA backbone. Back-biting reactions lead to the formation of macrocycles and thereby result in very broad or multimodal molecular weight distributions. Interestingly, some lithium complexes bearing bulky bis(phenolate) ligands[35] have recently been reported as efficient catalysts for the ring-opening polymerization of L-LA where, in the presence of benzyl alcohol as the chain transfer agent, high catalytic activities were observed in a living behavior.

Derivatives **1**, **8**, **13**, and **14** were also examined for the production of poly(lactides) (PLAs) (Table 3). Lithium salt **1** proved to be an active catalyst for the polymerization of L-lactide at 110 °C in toluene without cocatalyst or activator (Table 3, entries 1–3). Polymerization of the optically active (*S*,*S*)-lactide (L-lactide) afforded 23% conversion of 100 equiv in 10 h, and the product had a low polydispersity index ($M_w/M_n = 1.28$, entry 1). On extending the reaction time up to 36 h, 92% of the monomer was transformed without a significant increase in

(30) For lactide polymerization initiated by discrete Zn-alkoxide complexes, see for example references 10, 11, and (a) Cheng, M.; Attygalle, A. B.; Lobkovsky, E. B.; Coates, G. W. *J. Am. Chem. Soc.* **1999**, *121*, 11583. (b) Chisholm, M. H.; Huffman, J. C.; Phomphrai, K. *Dalton Trans.* **2001**, 222. (c) Jensen, T. R.; Schaller, C. P.; Hillmyer, M. A.; Tolman, W. B. *J. Organomet. Chem.* **2005**, *690*, 5881.

(31) (a) Sánchez-Barba, L. F.; Hughes, D. L.; Humphrey, S. M.; Bochmann, M. *Organometallics* **2005**, *24*, 3792. (b) Sánchez-Barba, L. F.; Hughes, D. L.; Humphrey, S. M.; Bochmann, M. *Organometallics* **2005**, *24*, 5329. (c) Sánchez-Barba, L. F.; Hughes, D. L.; Humphrey, S. M.; Bochmann, M. *Organometallics* **2006**, *25*, 1012.

(32) Lian, B.; Thomas, C. M.; Casagrande, O. L., Jr.; Lehmann, C. W.; Roisnel, T.; Carpentier, J.-F. *Inorg. Chem.* **2007**, *46*, 328.

(33) (a) Sarazin, Y.; Schormann, M.; Bochmann, M. *Organometallics* **2004**, *23*, 3296. (b) Sarazin, Y.; Howard, R. H.; Hughes, D. L.; Humphrey, S. M.; Bochmann, M. *Dalton Trans.* **2006**, 340.

(34) (a) Kricheldorf, H. R.; Saunder, K. *Makromol. Chem.* **1990**, *191*, 1057. (b) Kasperczyk, J. E. *Macromolecules* **1995**, *28*, 3937. (c) Xie, W.; Chen, D.; Fan, X.; Li, J.; Wang, P. G.; Cheng, H. N.; Nickol, R. G. *J. Polym. Sci., Part A: Polym. Chem.* **1999**, *37*, 3486. (d) Kasperczyk, J. E.; Bero, M. *Polymer* **2000**, *41*, 391.

(35) (a) Ko, B.-T.; Lin, C.-C. *J. Am. Chem. Soc.* **2001**, *123*, 7973. (b) Hsueh, M.-L.; Huang, B.-H.; Wu, J.; Lin, C.-C. *Macromolecules* **2005**, *38*, 9482. (c) Huang, B.-H.; Ko, B.-T.; Athar, T.; Lin, C.-C. *Inorg. Chem.* **2006**, *45*, 7348. (d) Chang, Y.-N.; Liang, L.-C. *Inorg. Chim. Acta* **2007**, *360*, 136. (e) Huang, C-A.; Chen, C-T. *Dalton Trans.* **2007**, 5561.

Table 4. Crystal Data and Summary of Data Collection and Refinement Details for 3, 8, 12, 15, and 16

	3	8	12	15	16
formula	$C_{18}H_{30}N_6$	$C_{20}H_{34}N_6Zn$	$C_{22}H_{38}N_6SiZn$	$C_{31}H_{56}N_6Zn$	$C_{32}H_{58}N_6Zn$
fw	330.48	423.90	480.04	578.19	592.21
T (K)	180(2)	180(2)	180(2)	180(2)	180(2)
λ, Å	0.71073	0.71073	0.71073	0.71073	0.71073
cryst syst	triclinic	triclinic	monoclinic	triclinic	monoclinic
space group	$P\bar{1}$	$P\bar{1}$	$C2/c$	$P\bar{1}$	$P2_1$
a (Å)	9.2756(7)	8.986(2)	18.559(3)	9.726(5)	9.874(1)
b (Å)	10.0456(8)	10.516(2)	18.300(3)	10.804(6)	17.786(2)
c (Å)	11.0945(9)	13.043(2)	16.155(3)	18.41(1)	10.841(1)
α (deg)	90.079(5)	94.295(3)	90	102.61(1)	90
β (deg)	106.283(5)	90.903(3)	103.559(3)	93.54(1)	116.015(2)
γ (deg)	96.837(5)	113.818(3)	90	114.20(1)	90
V (Å^3)	984.6(1)	1122.9(4)	5333.8(14)	1697(2)	1711.1(3)
Z	2	2	8	2	2
$D_{calcd.}$ (Mg/m^3)	1.115	1.254	1.196	1.132	1.149
μ (mm^{-1})	0.070	1.109	0.985	0.751	0.746
F(000)	360	452	2048	628	644
cryst size (mm^3)	0.35 × 0.34 × 0.14	0.40 × 0.25 × 0.22	0.61 × 0.24 × 0.07	0.54 × 0.34 × 0.23	0.42 × 0.33 × 0.27
θ range for data collection (deg)	2.04 to 25.00	2.13 to 25.00	2.26 to 23.22	2.15 to 28.00°.	2.09 to 27.29°
index ranges	$-11 \le h \le 11$	$-10 \le h \le 10$	$-20 \le h \le 20$	$-12 \le h \le 12$	$-10 \le h \le 12$
	$-11 \le k \le 11$	$-12 \le k \le 12$	$-19 \le k \le 20$	$-11 \le k \le 14$	$-22 \le k \le 22$
	$-13 \le l \le 13$	$-15 \le l \le 15$	$-17 \le l \le 16$	$-24 \le l \le 24$	$-9 \le l \le 13$
no. obsd reflns [$I > 2\sigma(I)$]	2057	3309	2897	5320	5151
no. of indep reflns	3395	3920	3745	8043	6558
	[R(int) = 0.0331]	[R(int) = 0.0389]	[R(int) = 0.0571]	[R(int) = 0.0650]	[R(int) = 0.0287]
no. of data/restraints/params	3395/0/229	3920/0/253	3745/0/303	8043/0/360	6558/1/370
goodness-of-fit on F^2	1.015	1.117	1.182	0.957	0.968
final R indices [$I > 2\sigma(I)$]	R1 = 0.0469	R1 = 0.0436	R1 = 0.0546	R1 = 0.0629	R1 = 0.0487
	wR2 = 0.1131	wR2 = 0.1095	wR2 = 0.1613	wR2 = 0.1486	wR2 = 0.0885
final R indices (all data)	R1 = 0.0783	R1 = 0.0514	R1 = 0.0719	R1 = 0.0920	R1 = 0.0682
	wR2 = 0.1323	wR2 = 0.1142	wR2 = 0.1736	wR2 = 0.1665	wR2 = 0.0971
largest diff peak and hole (e Å^{-3})	0.164 and −0.175	0.497 and −0.459	0.901 and −0.442	0.402 and −0.687	0.559 and −0.776

molecular weight distribution (M_w/M_n = 1.35, entry 2). When the polymerization was carried out in bulk conditions, 90% of the polymer was recovered after 45 min with a broader polydispersity (M_w/M_n = 1.45, entry 3). The polymerization occurs without epimerization reactions at the chiral centers, as evidenced by the homonuclear decoupled ^{1}H NMR spectrum, which reveals only a single resonance at δ 5.16 ppm in the methine region. The high levels of crystallinity and isotacticity in the polymer microstructure were also manifested by the high values of T_m (in the range 154–156 °C).[36] End group analysis revealed that the heteroscorpionate ligand was not attached to the end of the chain, in a similar way commented previously in the polymerization processes of ϵ-caprolactone (see above). Interestingly, Chisholm et al.[37] are currently designing group 1 metal and thallium tris(pyrazolyl)hydroborate complexes as transfer agents for the formation of LCaOR initiators for the ring-opening polymerization of lactides. However, as far as we are aware, these compounds have not yet been tested directly for polymerization purposes.

Alkyl zinc complexes **13** and **14** were found to be much less active than the lithium derivative **1**, as previously observed for Chisholm et al.[38] between binolate lithium and zinc complexes, and for the production of PCL (Table 3, entries 4–7). Thus, after 48 h in toluene at 110 °C, 81% of the monomer was converted in the case of **13** and the material had a narrow polydispersity index (M_w/M_n = 1.08, entry 6). The polymerization occurs without epimerization reactions and affords highly crystalline, isotactic polymers with high T_m values in the temperature range 162–165 °C.[36] The low level of stereochemical imperfections is also revealed in the poly(L-lactide) with M_n > 10 000 (entry 6), for which the optical activity remains almost constant, $[\alpha]_D^{22}$ = 144.[12b] The good level of control afforded by this initiator in the polymerization of L-lactide is further exemplified by the narrow molecular weight distributions, whereas it was not possible to establish linear correlations between M_n and percentage conversion characteristic of living propagations, a situation in contrast to the living behavior previously observed in magnesium[17] derivatives.

Initiators **8**, **13**, and **14** were also tested for the polymerization of *rac*-lactide, an equimolecular mixture of the D- and L-lactide, in toluene at 110 °C (Table 3, entries 9–14). Derivative **13** gave 33% conversion of 100 equiv after 24 h (entry 10) and produced low molecular weight material with a narrow polydispersity (M_w = 5400, M_w/M_n = 1.08). Extension of the reaction time to 48 h increased the activity, with conversion rising to 71% without a significant increase in polydispersity (M_w/M_n = 1.13, entry 11), while under bulk conditions 61% of the polymer was recovered after 45 min with a broader polydispersity (M_w/M_n = 1.43, entry 12). We attribute this broad molecular weight distribution to gradual catalyst decomposition on increasing the temperature and a small degree of transesterification and/or slow initiation relative to propagation; that is, the k_p/k_i ratio is not ultimately favorable. In all cases (entries 10–14), low melting materials were obtained with the T_m ranging from 125 to 134 °C. As far as we are aware, examples of zinc alkyl initiators[39,33b,11] have not been reported to act as active single-site catalysts for the ROP of *rac*-lactide. However, excellent tris(pyrazolyl)hydrobo-

(36) (a) Radano, C. P.; Baker, G. L.; Smith, M. R. *J. Am. Chem. Soc.* **2000**, *122*, 1552. (b) Zhong, Z.; Dijkstra, J. P.; Feijen, J. *J. Am. Chem. Soc.* **2003**, *125*, 11291.

(37) (a) Chisholm, M. H.; Gallucci, J. C.; Yaman, G. *Chem. Commun.* **2006**, 1872. (b) Chisholm, M. H.; Gallucci, J. C.; Yaman, G. *Inorg. Chem.* **2007**, *46*, 8676.

(38) Chisholm, M. H.; Lin, C.-C.; Gallucci, J. C.; Ko, B.-T. *Dalton Trans.* **2003**, 406.

(39) Duda, A.; Penczek, S. *Polymers from Renewable Resources: Biopolyesters and Biocatalysts*; Scholz, C., Gross, R. A., Eds.; ACS Symposium Series 764; American Chemical Society: Washington, DC, 2000; p 160.

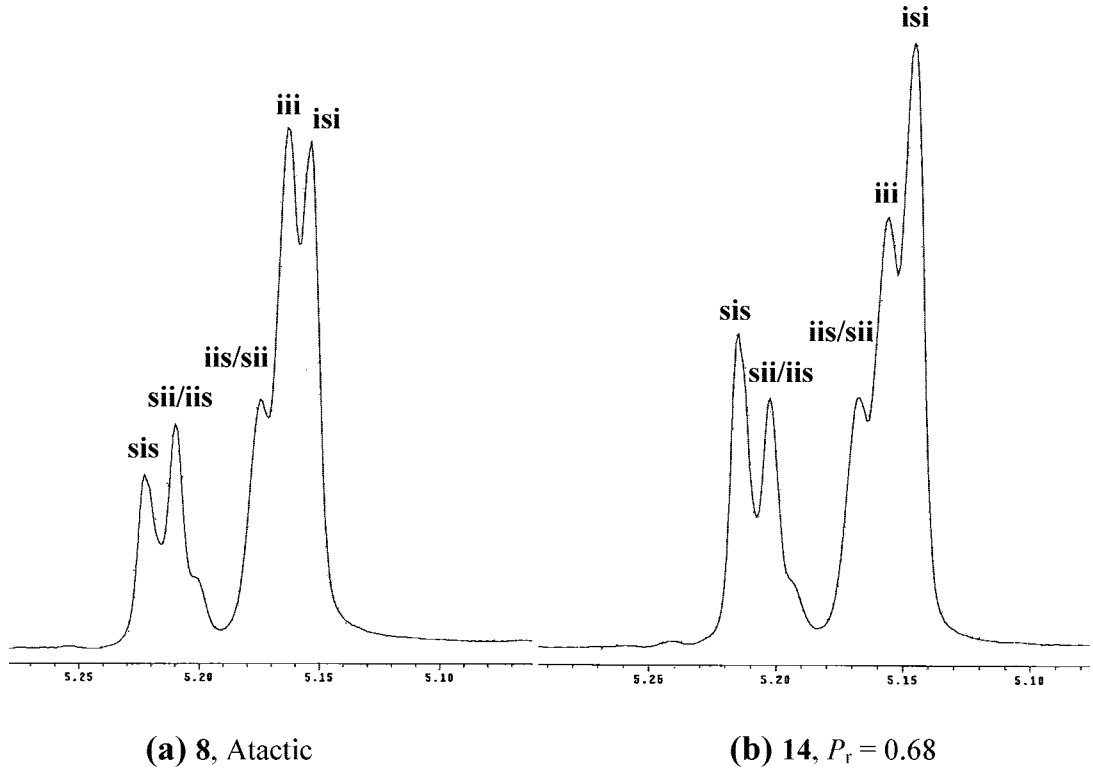

Figure 6. ^{1}H NMR spectrum (500 MHz, 298 K, $CDCl_3$) of the homodecoupled C*H* resonance of poly(*rac*-lactide) prepared in toluene at 110 °C using (a) [Zn(CH_2CH_3)(tbpamd)] (**8**) and (b) [Zn(CH_2CH_3)(tbp^{t}amd)] (**14**) as initiators. The tacticity of the polymer was assigned using the methine signals as described by Hillmyer and co-workers.[45]

rate-based alkoxide zinc complexes have been reported[12b] to produce poly(lactides) with high stereocontrol in the polymer microstructures as well as narrow molecular weight distributions. To circumvent this limitation, and in a similar way to the magnesium systems,[17] we decided to transform "*in situ*" the alkyl group by alcoholysis to give an isopropoxide group that would be a more suitable mimic of the putative propagating alkoxide species. In agreement with this assumption, addition of 1 equiv of HO^{i}Pr to the precatalyst **14** resulted in a significant increase in activity, as previously observed for magnesium, with the conversion rising from 63% to 89% and a slightly broader molecular weight distribution ($M_w/M_n = 1.23$, entry 14) obtained under otherwise identical conditions. The polymer characteristics remained unchanged. PLA end group analysis showed in all cases that, as for PCL initiated by alkyl zinc complexes, the polymerization was initiated by nucleophilic attack of alkyl/alkoxide on lactide.

Microstructural analysis of the poly(*rac*-lactide) by ^{1}H NMR spectroscopy revealed that **13** and **14** exert an interesting influence on the tacticity of the resulting polymer in comparison with the less sterically congested heteroscorpionate alkyl zinc **8** and analogous magnesium initiators reported by our group.[17] In these cases the heterotactic tetrads *isi* and *sis* were markedly enhanced as a result of the preference of the consecutive alternate insertion of the L- and D-lactide units into the growing chain (Figure 6). Recently, Chisholm and co-workers have shown that calcium catalysts containing bulky tris(pyrazolyl)-hydroborate ligands and phenolate or N($SiMe_3$)$_2$ initiators polymerize *rac*-lactide with a very high degree of heteroactivity in THF (90% of heterotactic PLA).[40] As observed in zinc complexes supported by tridentate Schiff base ligands[41] and calcium analogues,[42] the polymerization for complex **14** with the bulky *tert*-butyl substituents in the R position of the pyrazolic rings resulted in appreciable preference for the heterotactic poly(lactide) from *rac*-lactide, showing a $P_r = 0.68$ for heterotactic junctions (*isi* + *sis*)[43,6c] as a result of a chain-end control and assistance of the [Zn(NNN)] fragment (Figure 6b). Replacement of the *tert*-butyl group with R = Me leads to production of atactic poly(lactide), as observed for complex **8** (Table 3, entry 9) and for the alkyl magnesium analogues[17] (Table 3, entry 8), under otherwise identical polymerization conditions (Figure 6a). This behavior during the propagation event is most probably a result of the low steric demand of the methyl substituents in both pyrazolic rings, which leads to sterically less congested, more flexible, and therefore less discriminating active centers to the incoming lactide, even in the permanent presence of the sterically hindered ^{t}Bu amidinate substituent in the position *cis* to the alkyl leaving group. It is worth noting that these results, while still modest and with scope for improvement, represent an interesting forward step in terms of inducing appreciable levels of stereocontrol by the aforementioned heteroscorpionate alkyl zinc initiators in comparison with previously reported results from our group.[17] More interestingly, the catalytic activity in the ROP of lactide for complexes **8**, **13**, and **14** proved to be higher than those previously observed for the analogous alkyl heteroscorpionate magnesium initiators[17] (Table 3, entry 8), probably as a result of possible symmetrical (Schlenk)[27,28] equilibrium competition and, therefore, the formation of sandwich species versus catalytic performance. These results differ from those reported by

(40) Chisholm, M. H.; Gallucci, J. C.; Phomphrai, K. *Inorg. Chem.* **2004**, *43*, 6717.

(41) Ying, H.; Tang, H.; Lin, C. *Macromolecules* **2006**, *39*, 3745.

(42) Darensbourg, D. J.; Wonsook, C.; Richers, C. P. *Macromolecules* **2007**, *40*, 3521.

Chisholm for zinc and magnesium alkoxides with tris(pyrazolyl)hydroborate ligands, [(Tp)ZnOR],[12b] and with bidentate chelating BDI ligands, [(BDI)Zn(O^{i}Pr)],[44] the catalytic activities of which show a reverse order.

In conclusion, we report here a facile synthesis of a new family of sterically hindered amidinate-based heteroscorpionate lithium salts [Li(tbp^{t}amd)(THF)] (**1**) and [Li(pbp^{t}amd)(THF)] (**2**) in very good yields. Subsequent hydrolysis of **1** and **2**, and the analogous less congested heteroscorpionates [Li(tbpamd)(THF)] and [Li(pbpamd)(THF)], produces the corresponding amidine ligands H-NNN (**3**–**6**). Furthermore, the reactions of **3**–**6** with 1 equiv of ZnR′$_2$ give new neutral heteroscorpionate alkyl zinc complexes of the type [Zn(R′)(NNN)] (**7**–**16**) through alkane elimination reactions. Quite unexpectedly, alkyl zinc complexes **7**–**16** do not undergo ligand redistribution, and the corresponding six-coordinate sandwich complexes are not formed, even in refluxing toluene or in a 2:1 stoichiometry (2 equiv vs Zn), as observed in similar heteroscorpionate magnesium and zinc systems.

The Lewis acidity of the heteroscorpionate lithium salts and alkyl nucleophilicity of the corresponding alkyl-containing zinc complexes are sufficient for attack on cyclic esters, meaning that the NNN lithium and alkyl zinc complexes can act as single-site initiators for the well-controlled polymerization of polar monomers over a wide range of temperatures. ϵ-Caprolactone is polymerized within minutes to give high-medium molecular weight polymers with medium broad values of polydispersities. Not surprisingly, the polymerization of LA occurs more slowly than that of CL but offers good control. L-Lactide afforded highly crystalline, isotactic PLA materials with medium molecular weights, polydispersities as narrow as $M_w/M_n = 1.05$, and very high melting temperatures ($T_m = 165$ °C). Propagation occurs without observable epimerization with both families of initiators. Additionally, the more sterically hindered initiators **13** and **14** promote the formation of heterotactic bias in the polymerization of *rac*-lactide, producing heterotactic-rich PLA with $P_r = 0.68$. End group analysis indicates that in the case of alkyl zinc heteroscorpionates the polymerization process is initiated by alkyl transfer to the monomer. New group 2 and 12 initiators are currently being synthesized in our laboratories, capable of inducing high levels of stereoselectivity, and producing this promising generation of polymeric architectures with novel microstructures and/or properties.

Experimental Section

General Procedures. All manipulations were performed under nitrogen using standard Schlenk techniques. Solvents were predried over sodium wire (toluene, *n*-hexane, THF, diethyl ether) or calcium hydride (dichloromethane) and distilled under nitrogen from sodium (toluene), sodium−potassium alloy (*n*-hexane), sodium−benzophenone (THF, diethyl ether), or calcium hydride (dichloromethane). Deuterated solvents were stored over activated 4 Å molecular sieves and degassed by several freeze–thaw cycles. Microanalyses were carried out with a Perkin-Elmer 2400 CHN analyzer. ^{1}H and ^{13}C NMR spectra were recorded on a Varian Mercury FT-400 spectrometer and referenced to the residual deuterated solvent. The NOESY-1D spectra were recorded on a Varian Inova FT-500 spectrometer with the following acquisition parameters: irradiation time 2 s and number of scans 256, using standard VARIANT-FT software. Two-dimensional NMR spectra were acquired using standard VARIANT-FT software and processed using an IPC-Sun computer. $ZnMe_2$, $ZnEt_2$, and $ZnCl_2$ were used as purchased (Aldrich). [Li(tbpamd)(THF)] and [Li(pbpamd)(THF)] were prepared according to the literature procedures.[16] 3,5-Di-*tert*-butylpyrazole was obtained by standard literature methods from 2,2,6,6-tetramethyl-3,5-heptandione and hydrazine monohydrate.[46] ϵ-Caprolactone was dried by stirring over fresh CaH_2 for 48 h, then distilled under reduced pressure and stored over activated 4 Å molecular sieves. L-Lactide and *rac*-lactide were sublimed twice, recrystallized from THF, and finally sublimed again prior to use. Gel permeation chromatography (GPC) measurements were performed on a Polymer Laboratories PL-GPC-220 instrument equipped with a PLgel 5 Å Mixes-C column, a refractive index detector, and a PD2040 light-scattering detector. The GPC column was eluted with THF at 40 °C at 1 mL/min and was calibrated using eight monodisperse polystyrene standards in the range 580−483 000 Da. PLA melting temperatures were measured using a melting point Block SMP 10. The sample was heated to 100 °C, then heated at a rate of 1 °C/min to 165 °C. The specific rotation $[\alpha]_D^{22}$ was measured at a concentration of 10 mg/mL in $CHCl_3$ at 22 °C on a ATAGO POLAX-2L polarimeter equipped with a Na lamp operating at 589 nm with a light path length of 10 cm.

Preparation of Compounds 1–16. Synthesis of [Li(tbp^{t}amd)(THF)] (1). In a 250 mL Schlenk tube, a solution of Bu^{n}Li (1.6 M in hexane) (1.68 mL, 2.68 mmol) was added dropwise to a cooled (−70 °C), stirred solution of bdtbpzm (1.00 g, 2.68 mmol) in THF (70 mL) and maintained at this temperature over a period of 2 h. *N*,*N*′-1-*tert*-Butyl-3-ethylcarbodiimide (0.39 mL, 2.68 mmol) was added dropwise to the suspension and stirred for 1 h at room temperature. The solvent was evaporated to dryness under reduced pressure, and the resulting sticky white product was recrystallized from hexane at −26 °C to give compound **1** as white crystals. Yield: 1.33 g, 86%. Anal. Calcd for $C_{34}H_{61}LiN_6O$: C, 70.79; H, 10.66; N, 14.57. Found: C, 70.64; H, 10.31; N, 14.72. ^{1}H NMR (C_6D_6, 297 K): δ 7.45 (s, 1 H, CH), 5.54 (s, 2 H, H^4), 3.58 (m, 4 H, THF), 2.48 (m, 2 H, N−CH_2CH$_3$), 1.74 (m, 4H, THF), 1.29 (m, 3 H, N−CH$_2$CH_3), 1.17 [bs, 45 H, N−C(CH_3)$_3$, ^{t}Bu^3, ^{t}Bu^5]. ^{13}C{^{1}H} NMR (C_6D_6, 297 K): δ 161.1 (N=C−N), 152.1, 140.2 (C$^{3\ or\ 5}$), 102.1 (C^4), 65.0 (CH), 66.5 (THF), 48.2 (*C*H$_2$CH$_3$), 39.4 [*C*(CH$_3$)$_3$], 39.2 (^{t}Bu^3), 39.0 (^{t}Bu^5), 38.3 [C(*C*H$_3$)$_3$], 24.1 (THF), 22.3 (CH$_2$*C*H$_3$). ^{7}Li NMR (C_6D_6, 297 K): δ 1.63 (s). Mass spectrum (FAB) (*m*/*z* assignment, % intensity): 498 [M$^+$ − THF − Li], 2.56.

Synthesis of [Li(pbp^{t}amd)(THF)] (2). The synthesis of **2** was carried out in an identical manner to **1**. Bu^{n}Li (1.6 M in hexane) (1.68 mL, 2.68 mmol), bdtbpzm (1.00 g, 2.68 mmol), *N*,*N*′-diisopropylcarbodiimide (0.39 mL, 2.68 mmol). Yield: 1.36 g, 88%. Anal. Calcd for $C_{34}H_{61}LiN_6O$: C, 70.79; H, 10.66; N, 14.57. Found: C, 71.03; H, 10.55; N, 14.35. ^{1}H NMR (C_6D_6, 297 K): δ 7.52 (s, 1 H, CH), 5.97 (s, 2 H, H^4), 4.23 [m, 1 H, C*H*(CH$_3$)$_2$], 3.82 [m, 1 H, C*H*(CH$_3$)$_2$], 3.57 (m, 4 H, THF), 1.69 (m, 4H, THF), 1.36 [d, 6 H, $^3J_{H-H} = 5.0$ Hz, CH(C*H*$_3$)$_2$], 1.27 [d, 6 H, $^3J_{H-H} = 5.0$ Hz, CH(C*H*$_3$)$_2$], 1.21 (bs, 36 H, ^{t}Bu^5, ^{t}Bu^3). ^{13}C{^{1}H} NMR (C_6D_6, 297 K): δ 161.2 (N=C−N), 151.8, 141.6 (C$^{3\ or\ 5}$), 100.5 (C^4), 68.3 (CH), 65.9 (THF), 48.2, 42.0 [*C*H(CH$_3$)$_2$], 32.1 (^{t}Bu^3), 32.3, 30.6 [CH(*C*H$_3$)$_2$], 30.5 (^{t}Bu^5), 25.4 (THF). ^{7}Li NMR (C_6D_6, 297 K): δ 1.61 (s). Mass spectrum (FAB) (*m*/*z* assignment, % intensity): 498 [M$^+$ − THF − Li], 3.12.

Synthesis of Htbpamd (3). In a 250 mL Schlenk tube, [Li(tbpamd)(THF)] (1.00 g, 2.54 mmol) was dissolved in diethyl ether (70 mL) and a saturated solution of NH_4Cl in water (40 mL) was added. The organic product was extracted with diethyl ether (3 × 30 mL), the organic layers were combined, dried over $MgSO_4$, and filtered, and the solvent was removed from the filtrate under reduced pressure to yield the title compound as a white solid. Yield:

(43) Cai, C.-X.; Amgoune, A.; Lehmann, C. W.; Carpentier, J.-F. *Chem. Commun.* **2004**, 330.

(44) Chisholm, M. H.; Gallucci, J. C.; Phomphrai, K. *Inorg. Chem.* **2005**, *44*, 8004.

(45) Zell, M. T.; Padden, B. E.; Paterick, A. J.; Thakur, K. A. M.; Kean, R. T.; Hillmyer, M. A.; Munson, E. J. *Macromolecules* **2002**, *35*, 7700.

(46) Wang, Z-X.; Qin, H-L. *Green Chem.* **2004**, *6*, 90.

0.76 g, 90%. Anal. Calcd for $C_{18}H_{30}N_6$: C, 65.42; H, 9.15; N, 25.43. Found: C, 65.52; H, 9.04; N, 25.47. ^{1}H NMR (C_6D_6, 297 K): δ 7.31 (s, 1 H, CH), 6.16 [bs, 1 H, *H*−NC(CH$_3$)$_3$], 5.53 (s, 2 H, H^4), 3.32 (q, 2 H, $^3J_{H-H}$ = 7.6 Hz, N-*CH*$_2$CH$_3$), 2.28 (s, 6 H, Me^5), 2.05 (s, 6 H, Me^3), 1.46 [s, 9 H, N−C(*CH*$_3$)$_3$], 1.23 (t, 3 H, $^3J_{H-H}$ = 7.6 Hz, N−CH$_2$*CH*$_3$). ^{13}C{^{1}H} NMR (C_6D_6, 297 K): δ 149.2 (N=C−N), 147.7, 141.2 (C$^{3\ or\ 5}$), 106.5 (C^4), 67.7 (CH), 51.0 (N−*C*H$_2$CH$_3$), 42.8 [N−*C*(CH$_3$)$_3$], 28.3 [N−C(*C*H$_3$)$_3$], 17.7 (N−CH$_2$*C*H$_3$), 13.6 (Me^5), 11.3 (Me^3).

Synthesis of Hpbpamd (4). The synthesis of **4** was carried out in an identical manner to **3**. [Li(pbpamd)(THF)] (1.00 g, 2.54 mmol). Yield: 0.74 g, 88%. Anal. Calcd for $C_{18}H_{30}N_6$: C, 65.42; H, 9.15; N, 25.43. Found: C, 65.22; H, 9.31; N, 25.08. ^{1}H NMR (C_6D_6, 297 K): δ 7.43 (s, 1 H, CH), 6.16 [bs, 1 H, *H*−NCH(CH$_3$)$_2$], 5.54 (s, 2 H, H^4), 4.24, 3.92 [2 sept, 1 H each, $^3J_{H-H}$ = 5.6 Hz, N−C*H*(CH$_3$)$_2$], 2.28 (s, 6 H, Me^5), 2.05 (s, 6 H, Me^3), 1.15 [d, 6 H, $^3J_{H-H}$ = 5.6 Hz, N−CH(*CH*$_3$)$_2$], 1.13 [d, 6 H, $^3J_{H-H}$ = 5.6 Hz, N−CH(C*H*$_3$)$_2$]. ^{13}C{^{1}H} NMR (C_6D_6, 297 K), δ 149.2 (N=C−N), 146.7, 141.2 (C$^{3\ or\ 5}$), 106.6 (C^4), 59.4 (CH), 47.8, 42.3 [N−*C*H(CH$_3$)$_2$], 22.2, 21.3 [N−CH(*C*H$_3$)$_2$], 13.6 (Me^5), 11.3 (Me^3).

Synthesis of Htbp^{t}amd (5). The synthesis of **5** was carried out in an identical manner to **3**. [Li(tbp^{t}amd)(THF)] (1.00 g, 1.73 mmol). Yield: 0.83 g, 96%. Anal. Calcd for $C_{30}H_{54}N_6$: C, 72.24; H, 10.91; N, 16.85. Found: C, 71.92; H, 10.64; N, 16.67. ^{1}H NMR (C_6D_6, 297 K): δ 7.44 (s, 1 H, CH), 6.03 (s, 2 H, H^4), 4.41 [bs, 1 H, *H*−NC(CH$_3$)$_3$], 3.45 (q, 2 H, $^3J_{H-H}$ = 7.2 Hz, N−C*H*$_2$CH$_3$), 1.54 [s, 9 H, N−C(C*H*$_3$)$_3$], 1.36 (s, 18 H, ^{t}Bu^5), 1.26 (t, 3 H, $^3J_{H-H}$ = 7.2 Hz, N−CH$_2$*CH*$_3$), 1.24 (s, 18 H, ^{t}Bu^3). ^{13}C{^{1}H} NMR (C_6D_6, 297 K): δ 159.1 (N=C−N), 152.4, 151.8 (C$^{3\ or\ 5}$), 102.9 (C^4), 69.6 (CH), 51.0 (N−*C*H$_2$CH$_3$), 43.1, 42.2 [N−*C*(CH$_3$)$_3$], 32.3 (N−CH$_2$*C*H$_3$), 31.2, 31.1 [*C*(CH$_3$)$_3$], 30.7 [N−C(*C*H$_3$)$_3$, ^{t}Bu^5], 28.6 (^{t}Bu^3).

Synthesis of Hpbp^{t}amd (6). The synthesis of **6** was carried out in an identical manner to **3**. [Li(pbp^{t}amd)(THF)] (1.00 g, 1.73 mmol). Yield: 0.85 g, 98%. Anal. Calcd for $C_{30}H_{54}N_6$: C, 72.24; H, 10.91; N, 16.85. Found: C, 72.44; H, 10.84; N, 16.66. ^{1}H NMR (C_6D_6, 297 K): δ 7.54 (s, 1 H, CH), 5.98 (s, 2 H, H^4), 4.20 [bs, 1 H, *H*−NCH(CH$_3$)2], 3.85 [m, 2 H, N−C*H*(CH$_3$)$_2$], 1.31 (s, 18 H, ^{t}Bu^5), 1.23 (s, 18 H, ^{t}Bu^3), 1.26, 1.16 [m, 12H, N−CH(*CH*$_3$)$_3$]. ^{13}C{^{1}H} NMR (C_6D_6, 297 K): δ 159.3 (N=C−N), 153.1, 151.8 (C$^{3\ or\ 5}$), 102.0 (C^4), 69.4 (CH), 54.3, 48.9 [N−*C*H(CH$_3$)$_2$], 32.7, 31.9 [*C*(CH$_3$)$_3$], 32.2, 31.8 [N−CH(*C*H$_3$)$_3$], 30.7 (^{t}Bu^5), 30.2 (^{t}Bu^3).

Synthesis of [Zn(Me)(tbpamd)] (7). In a 250 mL Schlenk tube, Htbpamd (1.00 g, 3.03 mmol) was dissolved in dry toluene (70 mL) and cooled to −70 °C. A solution of $ZnMe_2$ (2.0 M in toluene) (1.51 mL, 3.03 mmol) was added, and the mixture was allowed to warm to room temperature and stirred during 2 h. The solvent was evaporated to dryness under reduced pressure to yield a sticky white product. The product was washed with hexane (30 mL) and recrystallized from toluene at −26 °C to give compound **7** as white crystals. Yield (1.09 g, 88%). Anal. Calcd for $C_{19}H_{32}N_6Zn$: C, 55.67; H, 7.87; N, 20.50. Found: C, 55.89; H, 7.68; N, 20.77. ^{1}H NMR (C_6D_6, 297 K): δ 7.32 (s, 1 H, CH), 5.23 (s, 2 H, H^4), 3.61 (q, 2 H, $^3J_{H-H}$ = 6.8 Hz, N−C*H*$_2$CH$_3$), 2.04 (s, 6 H, Me^5), 1.91 [s, 9 H, N−C(C*H*$_3$)$_3$], 1.51 (t, 3 H, $^3J_{H-H}$ = 6.8 Hz, N−CH$_2$C*H*$_3$), 1.47 (s, 6 H, Me^3), 0.15 (s, 3 H, ZnC*H*$_3$). ^{13}C{^{1}H} NMR (C_6D_6, 297 K), δ 155.0 (N=C−N), 149.3, 139.3 (C$^{3\ or\ 5}$), 106.7 (C^4), 54.1 (CH), 44.1 (N−*C*H$_2$CH$_3$), 38.2 [N−*C*(CH$_3$)$_3$], 31.3 [N−C(*C*H$_3$)$_3$], 28.3 (N−CH$_2$*C*H$_3$), 12.7 (Me^5), 10.2 (Me^3), 0.6 (Zn*C*H$_3$).

Synthesis of [Zn(Et)(tbpamd)] (8). The synthesis of **8** was carried out in an identical manner to **7**. $ZnEt_2$ (1.0 M in hexane) (3.03 mL, 3.03 mmol), Htbpamd (1.00 g, 3.03 mmol). Yield (1.05 g, 82%). Anal. Calcd for $C_{20}H_{34}N_6Zn$: C, 56.67; H, 8.08; N, 19.82. Found: C, 56.89; H, 8.28; N, 20.18. ^{1}H NMR (C_6D_6, 297 K): δ 7.20 (s, 1 H, CH), 5.23 (s, 2 H, H^4), 3.59 (q, 2 H, $^3J_{H-H}$ = 7.2 Hz, N−C*H*$_2$CH$_3$), 2.07 (s, 6 H, Me^5), 1.91 (t, 3 H, $^3J_{H-H}$ = 8.0 Hz, ZnCH$_2$C*H*$_3$), 1.88 [s, 9 H, N−C(C*H*$_3$)$_3$], 1.50 (s, 6 H, Me^3), 1.49 (t, 3 H, $^3J_{H-H}$ = 7.2 Hz, N−CH$_2$C*H*$_3$), 0.94 (q, 2 H, $^3J_{H-H}$ = 8.0 Hz, ZnC*H*$_2$CH$_3$). ^{13}C{^{1}H} NMR (C_6D_6, 297 K): δ 154.0 (N=C−N), 148.8, 135.8 (C$^{3\ or\ 5}$), 106.2 (C^4), 59.0 (CH), 53.7 (N−*C*H$_2$CH$_3$), 44.1 [N−*C*(CH$_3$)$_3$], 31.2 [N−C(*C*H$_3$)$_3$], 19.5 (N−CH$_2$*C*H$_3$), 13.8 (ZnCH$_2$*C*H$_3$), 12.9 (Me^5), 10.3 (Me^3), 0.8 (Zn*C*H$_2$CH$_3$).

Synthesis of [Zn(CH$_2$SiMe$_3$)(tbpamd)] (9). Compound **9** was made in a one-pot reaction. A solution of [Li(CH$_2$SiMe$_3$)] (0.62 g, 6.60 mmol) in diethyl ether (50 mL) was added to a cooled (−40 °C), stirred suspension of $ZnCl_2$ (0.45 g, 3.30 mmol) in diethyl ether (30 mL) in a 250 mL Schlenk tube. The mixture was allowed to warm to room temperature and stirred for 1 h. An increasing turbidity developed, and this finally led to the formation of a white suspension. The suspension was filtered and the filtrate, corresponding to Zn(CH$_2$SiMe$_3$)$_2$, was added to a precooled (−20 °C) solution of Htbpamd (1.09 g, 3.30 mmol) in diethyl ether. The mixture was stirred at this temperature for 2 h. The volatiles were removed, and the resulting sticky white solid was recrystallized from toluene to give the title compound **9** as white crystals. Yield: 1.27 g, 80%. Anal. Calcd for $C_{22}H_{40}N_6SiZn$: C, 54.81; H, 8.36; N, 17.43. Found: C, 54.66; H, 8.16; N, 17.55. ^{1}H NMR (C_6D_6, 297 K): δ 7.22 (s, 1 H, CH), 5.30 (s, 2 H, H^4), 3.62 (q, 2 H, $^3J_{H-H}$ = 7.2 Hz, N−*CH*$_2$CH$_3$), 2.15 [s, 9 H, N−C(C*H*$_3$)$_3$], 1.91 (s, 6 H, Me^5), 1.73 (s, 6 H, Me^3), 1.52 (t, 3 H, $^3J_{H-H}$ = 7.2 Hz, N−CH$_2$C*H*$_3$), 0.54 (s, 9 H, ZnCH$_2$Si*Me*$_3$), −0.17 (s, 2 H, ZnC*H*$_2$SiMe$_3$). ^{13}C{^{1}H} NMR (C_6D_6, 297 K): δ 153.9 (N=C−N), 150.4, 143.6 (C$^{3\ or\ 5}$), 106.4 (C^4), 67.8 (CH), 54.0 (N−*C*H$_2$CH$_3$), 44.0 [N−*C*(CH$_3$)$_3$], 31.5 [N−C(*C*H$_3$)$_3$], 19.5 (N−CH$_2$*C*H$_3$), 17.8 (Me^5), 14.3 (Me^3), 4.2 (ZnCH$_2$Si*Me*$_3$), −6.7 (Zn*C*H$_2$SiMe$_3$).

Synthesis of [Zn(Me)(pbpamd)] (10). The synthesis of **10** was carried out in an identical manner to **7**. $ZnMe_2$ (2.0 M in toluene) (1.51 mL, 3.03 mmol), Hpbpamd (1.00 g, 3.03 mmol). Yield: 0.96 g, 78%. Anal. Calcd for $C_{19}H_{32}N_6Zn$: C, 55.67; H, 7.87; N, 20.50. Found: C, 55.78; H, 7.99; N, 20.10. ^{1}H NMR (C_6D_6, 297 K): δ 7.34 (s, 1 H, CH), 5.24 (s, 2 H, H^4), 4.92 [sept, 1 H, $^3J_{H-H}$ = 6.4 Hz, C*H*(CH$_3$)$_2$], 3.87 [sept, 1 H, $^3J_{H-H}$ = 6.4 Hz, C*H*(CH$_3$)$_2$], 2.06 (s, 6 H, Me^5), 1.74 (s, 6 H, Me^3), 1.52 [d, 6 H, $^3J_{H-H}$ = 6.4 Hz, CH(C*H*$_3$)$_2$], 1.38 [d, 6 H, $^3J_{H-H}$ = 6.4 Hz, CH(C*H*$_3$)$_2$], 0.16 (s, 3 H, ZnC*H*$_3$). ^{13}C{^{1}H} NMR (C_6D_6, 297 K): δ 152.0 (N=C−N), 148.8, 139.2 (C$^{3\ or\ 5}$), 105.9 (C^4), 57.4 (CH), 49.8 [N−*C*H(CH$_3$)$_2$], 45.0 [N−*C*H(CH$_3$)$_2$], 27.6 [N−CH(*C*H$_3$)$_2$], 24.9 [N−CH(*C*H$_3$)$_2$], 12.7 (Me^5), 10.3 (Me^3), −0.4 (Zn*C*H$_3$).

Synthesis of [Zn(Et)(pbpamd)] (11). The synthesis of **11** was carried out in an identical manner to **7**. $ZnEt_2$ (1.0 M in hexane) (3.03 mL, 3.03 mmol), Hpbpamd (1.00 g, 3.03 mmol). Yield (1.05 g, 82%). Anal. Calcd for $C_{20}H_{34}N_6Zn$: C, 56.67; H, 8.08; N, 19.82. Found: C, 56.78; H, 8.01; N, 19.33. ^{1}H NMR (C_6D_6, 297 K): δ 7.30 (s, 1 H, CH), 5.23 (s, 2 H, H^4), 4.85 [sept, 1 H, $^3J_{H-H}$ = 5.2 Hz, *CH*(CH$_3$)$_2$], 3.84 [sept, 1 H, $^3J_{H-H}$ = 5.2 Hz, *CH*(CH$_3$)$_2$], 2.04 (s, 6 H, Me^3), 1.91 (t, 3 H, $^3J_{H-H}$ = 8.0 Hz, ZnCH$_2$C*H*$_3$), 1.73 (s, 6 H, Me^5), 1.46 [d, 6 H, $^3J_{H-H}$ = 5.2 Hz, CH(C*H*$_3$)$_2$], 1.31 [d, 6 H, $^3J_{H-H}$ = 5.2 Hz, CH(C*H*$_3$)$_2$], 0.94 (t, 2 H, $^3J_{H-H}$ = 8.0 Hz, ZnC*H*$_2$CH$_3$). ^{13}C{^{1}H} NMR (C_6D_6, 297 K): δ 152.2 (N=C−N), 148.8, 139.6 (C$^{3\ or\ 5}$), 106.0 (C^4), 57.5 (CH), 49.9 [N−*C*H(CH$_3$)$_2$], 44.8 [N−*C*H(CH$_3$)$_2$], 27.7 [N−CH(*C*H$_3$)$_2$], 24.9 [N−CH(*C*H$_3$)$_2$], 14.1 (ZnCH$_2$*C*H$_3$), 12.9 (Me^5), 10.4 (Me^3), −0.7 (Zn*C*H$_2$CH$_3$).

Synthesis of [Zn(CH$_2$SiMe$_3$)(pbpamd)] (12). The synthesis of **12** was carried out in an identical manner to **9**. [Li(CH$_2$SiMe$_3$)] (0.62 g, 6.60 mmol), $ZnCl_2$ (0.45 g, 3.30 mmol), Hpbpamd (1.09 g, 3.30 mmol). Yield: 0.96 g (1.24 g, 78%). Anal. Calcd for $C_{22}H_{40}N_6SiZn$: C, 54.81; H, 8.36; N, 17.43. Found: C, 54.78; H, 8.64; N, 17.10. ^{1}H NMR (C_6D_6, 297 K): δ 7.30 (s, 1 H, CH), 5.24 (s, 2 H, H^4), 4.89 [m, 1 H, C*H*(CH$_3$)$_2$], 3.88 [m, 1 H, C*H*(CH$_3$)$_2$], 2.10 (s, 6 H, Me^5), 1.74 (s, 6 H, Me^3), 1.49 [d, 6 H, $^3J_{H-H}$ = 5.6 Hz, CH(C*H*$_3$)$_2$], 1.34 [d, 6 H, $^3J_{H-H}$ = 5.6 Hz, CH(C*H*$_3$)$_2$], 0.11 (s, 9 H, ZnCH$_2$Si*Me*$_3$), −0.59 (s, 2 H, ZnC*H*$_2$SiMe$_3$). ^{13}C{^{1}H} NMR (C_6D_6, 297 K): δ 154.2 (N=C−N), 150.8, 144.3 (C$^{3\ or\ 5}$), 107.3

(C^4), 65.9 (CH), 49.3, 47.1 [N−*C*H(CH_3)$_2$], 25.2, 24.4 [N−CH(*C*H$_3$)$_2$], 15.6 (Me^5), 13.3 (Me^3), 3.9 ($ZnCH_2SiMe_3$), −7.3 ($ZnCH_2SiMe_3$).

Synthesis of [Zn(Me)(tbp^{t}amd)] (13). The synthesis of **13** was carried out in an identical manner to **7**, except compound **13** was recrystallized from hexane. $ZnMe_2$ (2.0 M in toluene) (1.00 mL, 2.00 mmol), Htbp^{t}amd (1.00 g, 2.00 mmol). Yield: 0.90 g, 78%. Anal. Calcd for $C_{31}H_{56}N_6Zn$: C, 64.39; H, 9.76; N, 14.53. Found: C, 64.58; H, 9.89; N, 14.20. ^{1}H NMR (C_6D_6, 297 K): δ 7.45 (s, 1 H, CH), 6.02 (s, 2 H, H^4), 3.50 (m, 2 H, N−C*H*$_2$CH$_3$), 1.54 [s, 9H, N−C(C*H*$_3$)$_3$], 1.33 (bs, 21 H, ^{t}Bu^3, N−CH$_2$C*H*$_3$), 1.28 (s, 18 H, ^{t}Bu^5), 0.18 (s, 3 H, ZnC*H*$_3$). ^{13}C{^{1}H} NMR (C_6D_6, 297 K): δ 153.8 (N=C−N), 153.1, 152.4 ($C^{3\ or\ 5}$), 102.0 (C^4), 69.7 (CH), 51.0 [N−*C*H$_2$CH$_3$)$_2$], 43.1 [N−*C*(CH$_3$)$_3$], 32.3, 32.1 [*C*(CH$_3$)$_3$], 30.8 (^{t}Bu^5), 30.6 (^{t}Bu^3), 28.6 [N−C(*C*H$_3$)$_3$], 17.6 (N−CH$_2$*C*H$_3$), −2.8 (Zn*C*H$_3$).

Synthesis of [Zn(Et)(tbp^{t}amd)] (14). The synthesis of **14** was carried out in an identical manner to **13**. $ZnEt_2$ (1.0 M in hexane) (2.00 mL, 2.00 mmol), Htbp^{t}amd (1.00 g, 2.00 mmol). Yield (0.97 g, 82%). Anal. Calcd for $C_{32}H_{58}N_6Zn$: C, 64.90; H, 9.87; N, 14.11. Found: C, 65.11; H, 9.66; N, 14.40. ^{1}H NMR (C_6D_6, 297 K): δ 7.45 (s, 1 H, CH), 6.03 (s, 2 H, H^4), 3.49 (q, 2 H, $^3J_{H-H}$ = 6.8 Hz, N−C*H*$_2$CH$_3$), 1.54 [s, 9H, N−C(C*H*$_3$)$_3$], 1.50 (t, 3H, $^3J_{H-H}$ = 6.4 Hz, ZnCH$_2$C*H*$_3$), 1.36 (s, 18 H, ^{t}Bu^5), 1.28 (t, 3 H, $^3J_{H-H}$ = 6.8 Hz, N−CH$_2$C*H*$_3$), 1.22 (s, 18 H, ^{t}Bu^3), 0.58 (q, 2 H, $^3J_{H-H}$ = 6.4 Hz, ZnC*H*$_2$CH$_3$). ^{13}C{^{1}H} NMR (C_6D_6, 297 K): δ 153.0 (N=C−N), 152.4, 151.9 ($C^{3\ or\ 5}$), 102.0 (C^4), 69.7(CH), 51.0 (N−*C*H$_2$CH$_3$), 43.1 [N−*C*(CH$_3$)$_3$], 32.3, 32.2 [*C*(CH$_3$)$_3$], 30.7 (^{t}Bu^5, ^{t}Bu^3), 30.1 (ZnCH$_2$*C*H$_3$), 28.6 [N−C(*C*H$_3$)$_3$], 17.6 (N−CH$_2$*C*H$_3$), 1.5 (Zn*C*H$_2$CH$_3$).

Synthesis of [Zn(Me)(pbp^{t}amd)] (15). The synthesis of **15** was carried out in an identical manner to **13**. $ZnMe_2$ (2.0 M in toluene) (1.00 mL, 2.0 mmol), Hpbp^{t}amd (1.00 g, 2.00 mmol). Yield (0.84 g, 73%). Anal. Calcd for $C_{31}H_{56}N_6Zn$: C, 64.39; H, 9.76; N, 14.53. Found: C, 63.98; H, 9.99; N, 14.42. ^{1}H NMR (C_6D_6, 297 K): δ 7.49 (s, 1 H, CH), 5.97 (s, 2 H, H^4), 4.17 [sept, 1 H, $^3J_{H-H}$ = 6.4 Hz, *CH*(CH$_3$)$_2$], 4.13 [sept, 1 H, $^3J_{H-H}$ = 6.4 Hz, *CH*(CH$_3$)$_2$], 1.37 (s, 18 H, ^{t}Bu^5), 1.36 (s, 18 H, ^{t}Bu^3), 1.28 [d, 6 H, $^3J_{H-H}$ = 6.4 Hz, CH(C*H*$_3$)$_2$], 1.21 [d, 6 H, $^3J_{H-H}$ = 6.4 Hz, CH(C*H*$_3$)$_2$], 0.22 (s, 3 H, ZnC*H*$_3$). ^{13}C{^{1}H} NMR (C_6D_6, 297 K): δ 161.9 (N=C−N), 154.3, 145.8 ($C^{3\ or\ 5}$), 102.0 (C^4), 78.0 (CH), 47.6 [N−*C*H(CH$_3$)$_2$], 47.1 [N−*C*H(CH$_3$)$_2$], 32.3, 32.1 [*C*(CH$_3$)$_3$], 31.0 (^{t}Bu^5), 30.2 (^{t}Bu^3), 26.8 [N−CH(*C*H$_3$)$_2$], 26.4 [N−CH(*C*H$_3$)$_2$], −4.7 (Zn*C*H$_3$).

Synthesis of [Zn(Et)(pbp^{t}amd)] (16). The synthesis of **16** was carried out in an identical manner to **13**. $ZnEt_2$ (1.0 M in hexane) (2.00 mL, 2.0 mmol), Hpbp^{t}amd (1.00 g, 2.00 mmol). Yield (0.90 g, 76%). Anal. Calcd for $C_{32}H_{58}N_6Zn$: C, 64.90; H, 9.87; N, 14.19. Found: C, 64.68; H, 9.59; N, 14.47. ^{1}H NMR (C_6D_6, 297 K): δ 7.45 (s, 1 H, CH), 5.99 (s, 2 H, H^4), 4.57 [sept, 1 H, $^3J_{H-H}$ = 6.4 Hz, *CH*(CH$_3$)$_2$], 4.26 [q, 1 H, $^3J_{H-H}$ = 6.4 Hz, *CH*(CH$_3$)$_2$], 1.86 (t, 3 H, $^3J_{H-H}$ = 6.8 Hz, ZnCH$_2$C*H*$_3$), 1.39 (s, 18 H, ^{t}Bu^5), 1.37 (s, 18 H, ^{t}Bu^3), 1.23 [d, 6 H, $^3J_{H-H}$ = 6.4 Hz, CH(C*H*$_3$)$_2$], 1.19 [d, 6 H, $^3J_{H-H}$ = 6.4 Hz, CH(C*H*$_3$)$_2$], 0.98 (q, 3 H, $^3J_{H-H}$ = 6.8 Hz, ZnC*H*$_2$CH$_3$). ^{13}C{^{1}H} NMR (C_6D_6, 297 K): δ 162.0 (N=C−N), 154.3, 145.8 ($C^{3\ or\ 5}$), 101.8 (C^4), 78.1 (CH), 47.2 [N−*C*H(CH$_3$)$_2$], 47.0 [N−*C*H(CH$_3$)$_2$], 32.3, 32.1 [*C*(CH$_3$)$_3$], 31.0 (^{t}Bu^5), 30.2 (^{t}Bu^3), 29.8 (ZnCH$_2$*C*H$_3$), 25.3 [N−CH(*C*H$_3$)$_2$], 25.1 [N-CH(*C*H$_3$)$_2$], 1.1 (Zn*C*H$_2$CH$_3$).

X-ray Crystallographic Structure Determination for Complexes 3, 8, 12, 15, and 16. A summary of crystal data collection and refinement parameters for all compounds is given in Table 4.

Single crystals of **3**, **8**, **12**, **15**, and **16** were mounted on a glass fiber and transferred to a Bruker X8 APEX II CCD-based diffractometer equipped with a graphite-monochromated Mo Kα radiation source (λ = 0.71073 Å). Data were integrated using SAINT,[47] and an absorption correction was performed with the program SADABS.[48] The software package SHELXTL version 6.12[49] was used for space group determination, structure solution, and refinement by full-matrix least-squares methods based on F^2. All non-hydrogen atoms were refined with anisotropic thermal parameters. Hydrogen atoms were placed using a "riding model" and included in the refinement at calculated positions.

Polymerization Procedures. Polymerizations of ϵ-caprolactone (CL) were carried out on a Schlenk line in a flame-dried round-bottom flask equipped with a magnetic stirrer. In a typical procedure, the initiator was dissolved in the appropriate amount of solvent, and temperature equilibration was ensured by stirring the solution for 15 min on a temperature bath. ϵ-CL was injected and polymerization times were measured from that point. Polymerizations were terminated by addition of acetic acid (5 vol %) in methanol. Polymers were precipitated in methanol, filtered, dissolved in THF, reprecipitated in methanol, and dried *in vacuo* to constant weight.

Polymerizations of L-lactide and *rac*-lactide (LA) were performed on a Schlenk line in a flame-dried round-bottomed flask equipped with a magnetic stirrer. The Schlenk tubes were charged in the glovebox with the required amount of *rac*-lactide and initiator, separately, and then attached to the vacuum line. The initiator and monomer were dissolved in the appropriate amount of solvent, and temperature equilibration was ensured in both Schlenk flasks by stirring the solutions for 15 min in a bath. The appropriate amount of initiator was added by syringe, and polymerization times were measured from that point. Polymerizations were stopped by injecting a solution of acetic acid (5 vol %) in methanol. Polymers were precipitated in methanol, filtered, dissolved in THF, reprecipitated in methanol, and dried *in vacuo* to constant weight.

Acknowledgment. We gratefully acknowledge financial support from the Ministerio de Educación y Ciencia (Dirección General de Investigación), Spain (Grant No. CTQ 2005-07918-CO2-02), Consejería de Educación, Comunidad de Madrid, Spain (Grant No. S-0505/PPQ/0328), and Consejería de Educación y Ciencia de Castilla-La Mancha, Spain (Grant No. PBI05-023). We are grateful to Prof. Manfred Bochmann from the UEA for the GPC measurement facilities.

OM701187S

(47) *SAINT+ v7.12a, Area-Detector Integration Program*; Bruker-Nonius AXS: Madison, WI, 2004.

(48) Sheldrick, G. M. *SADABS version 2004/1, a Program for Empirical Absorption Correction*; University of Göttingen: Göttingen, Germany, 2004.

(49) *SHELXTL-NT version 6.12, Structure Determination Package*; Bruker-Nonius AXS: Madison, WI, 2001.